Master Thesis in Geographical Information Science nr 154

Where there is road, there is fire (influence): An exploratory study on the influence of roads in the spatial patterns of Swedish wildfires of 2018

Gabriel Romeo Ferriols Pavico

2023
Department of
Physical Geography and Ecosystem Science
Centre for Geographical Information Systems
Lund University
Sölvegatan 12
S-223 62 Lund
Sweden

Gabriel Romeo Ferriols Pavico (2023). Where there is road, there is fire (influence): An exploratory study on the influence of roads in the spatial patterns of Swedish wildfires of 2018.

Master degree thesis, 30 credits in Master in Geographical Information Science
Department of Physical Geography and Ecosystem Science, Lund University

Where there is road, there is fire (influence): An exploratory study on the influence of roads in the spatial patterns of Swedish wildfires of 2018

Gabriel Romeo Ferriols Pavico
Master thesis, 30 credits, in Geographical Information Sciences

Anders Ahlström
Department of Physical Geography and Ecosystem Science
Lund University

Acknowledgments

It takes a village to raise a child. I could say that the same is true in the creation of this thesis. This is to everyone who have had an impact on me throughout this master's programme and in the completion of this thesis project.

Anders Ahlström, my thesis mentor. Thank you so much for pushing my work towards greatness. The birthing process of the thesis was tough, but with your dedication and engagement, it allowed me to strive for the best and try to go beyond my preconceived limits. I would also like to express my gratitude to Helena Elvén Eriksson and David Tenenbaum for taking the time to review the study and your engagement as examiners in the presentation of the thesis.

To my classmates in this programme, thank you very much for your presence. With the friendships and the camaraderie made, I did not feel alone in the struggles of doing this distance programme. Shout out to Ben, Sara, and Felix!

To Antonio Marañon for your statistical expertise. For your patience with all my questions, and the Saturdays working together. To Lucy and the rest of my Filipino family in Lund and Skåne for all the support and encouragement you've given.

Kestrel Quiambao and Lui Palmares for your willingness to proofread this thesis. Thank you for doing your best and squeezing this enormous task in your schedule. Also, to Mathias Johansson who has provided some pragmatic feedback on my results.

To my beloved Cem, thank you for allowing me to have the space for my personal and professional growth amidst the pandemic. For always believing in me and your tireless dedication in teaching coding to me during the python and algorithms courses. Thank you as well for the Swedish translation of the abstract. This is also your thesis.

Lastly, to my mother Joy, my second mother Rose and to my family, this is also for you.

Abstract - EN

This study focuses on the Swedish wildfire season of 2018, when the country incurred ten times more than the average burnt area that occurred in previous years. The study aims to address a broad research question: How do roads influence the size of a fire's burned area? This study fills the gap in research on the effects of roads in the spatial patterns of wildfires. Moreover, the research hopes to include the influence of roads in the narrative of wildfire patterns.

Among other statistical methods, multivariate regression analysis was ultimately used to answer the research question. Looking at road, landcover, proximity to towns, temperature and fire weather index (FWI), it was found that the parcel sizes of forest and open landscapes influence the average burnt area of a fire. An increase of mean forest area coincides with larger fires, while the inverse is seen for open landscapes. This, in turn, suggests that roads act as fuel breaks and suppression access points by fragmenting forests.

A second method that measured the ratio of a fire's perimeter conforming to the contours of the roads supports the results of the multivariate method above. Of the fires that had edges that conformed to roads, this corresponds to 95% of the total fire area in 2018. An average of 26.7% of the ratio of road conformity was seen in these fires. The increase in conformity percentage led to smaller fire areas. The model created in this method tested what drives the amount of road conformity of fires. The amount of road density and total forest area were statistically significant in driving the conformity of fire perimeter to roads.

Keywords: Geography, GIS, Wildfire, Fire Spatial Patterns, Road, Conformity, FWI

Advisor: Anders Ahlström
Master degree project 30 credits in Geographical Information Sciences, 2023
Department of Physical Geography and Ecosystem Science, Lund University
Thesis nr 154

Abstract - SV

Studiens fokus är på skogsbränderna i Sverige år 2018, då tio gånger mer markyta påverkades av bränder än genomsnittet under föregående år. Syftet med studien är att undersöka en bred forskningsfråga: Hur påverkas den brända ytan från en löpeld av vägar? Studien bygger på tidigare forskning om hur spridningen av löpeld påverkas av vägar.

Bland olika statistiska metoder valdes slutligen multivariat regressionsanalys för att besvara forskningsfrågan. Genom att ta hänsyn till vägar, marktäcke, närheten till bebyggelse, temperatur samt FWI (Fire Weather Index) kunde ett samband finnas mellan storleken på skogspartier och den genomsnittliga ytan av en brand. En ökning av genomsnittsytan av skogspartier korrelerar med en större brand, medan motsatsen kan ses för öppna landskap. Detta tyder på att vägar dels ökar framkomligheten för brandbekämpning, och dels fungerar som en broms för spridningen av eld genom att dela upp skogen i mindre partier.

En annan metod mäter hur stor andel av en brands ytterkant följer en väg, och den här metoden stödjer resultaten från den multivariata metoden. Bränder vars perimeter följde vägar utgjorde 95% av den sammanlagda ytan som brann år 2018. För dessa bränder sammanföll i genomsnitt 26,7% av ytterkanten med en väg. En högre andel kan ses korrelera med en mindre brandyta. Modellen som skapades för den här metoden undersökte vad som driver brändernas anpassning till vägar. Vägtätheten och den totala skogsarealen var statistiskt signifikanta när det gällde hur mycket brandperimetrar följer vägar.

Nyckelord: Geografi, GIS, Skogsbränder, Spatiala brandmönster, Vägar, Konformitet

Handledare: Anders Ahlström
Examensarbete för masterexamen 30 hp i geografisk informationsvetenskap, 2023
Institutionen för naturgeografi och ekosystemvetenskap, Lunds universitet
Examensarbete nr 154

Table of Contents

List of Figures

List of Tables

1 Introduction

1.1 On Wildfires and Roads

Wildfires are a phenomenon where fires occur in an uncontrolled way in natural environments such as forests, wetlands, and open landscapes. Wildfire events could either start off as natural occurrences or through anthropogenic causes (Narayanaraj and Wimberly, 2012). As a natural process in the ecosystem, the effects of wildfires could act as a renourishment or reinvigoration of vegetation and affect the spread of species (Houghton, 2015, p. 222; World Wildlife Fund for Nature and Boston Consulting Group, 2020).

As an effect of climate change, an EU report predicts that as an effect of climate change, in 2022, Europe could experience a longer drought period up until November, thus making landscapes vulnerable to wildfires (Cook, 2022). Not only are humans affecting wildfire occurrences via climate change (IPCC, 2007), but also through the direct ignition of fires themselves. In a report by the WWF, 75% of global wildfires in 2020 were ignited by human activity (World Wildlife Fund for Nature and Boston Consulting Group, 2020). As wildfires pose as a threat to property and health, humans have also taken part in the direct suppression of these events.

As another anthropogenic cause, through the course of development of urban and sub-urban areas, there is a necessity to reappropriate land to expand the road network for interconnectivity of an area to the rest of the development (Dewberry, 2008, p. 3; Wachs and Schofer, 1969). As a country develops, roads are essential to efficiently connect towns from each other. This is true in agro-industrial areas such as fields and forests where road access is essential for the transportation of labour and of goods for industrial purposes (Spinelli and Marchi, 1998, cited in Laschi *et al.*, 2019). Roads are also essential in leisure activities for people to get to an area via a vehicle and eventually by foot to some attractions (Newsome, Moore and Dowling, 2013, pp. 125-129). And in this process, roads exist in these landscapes, cutting through forest land, wetland, and other types of landscapes.

In the summer of 2018, a government report detailed that Sweden experienced several wildfires where about 25 000 hectares of forest land were burnt, or in other words less than 0.1% (of 28 million hectares total) of the country's total forest area (SOU, 2019, p. 13). The same report showed that the burnt area in 2018 was ten times larger than the annual average incurred in

2000 to 2017, where the affected areas account for 2 600 hectares annually (pp. 49-50). Of the total 25 000 hectares, 18 000 hectares (72 percent) of the wildfires happened during the weekend of July 14 and 15 (p. 110), with the counties of Gävleborg, Jämtland and Dalarna being affected the most (Krisinformation.se, 2018).

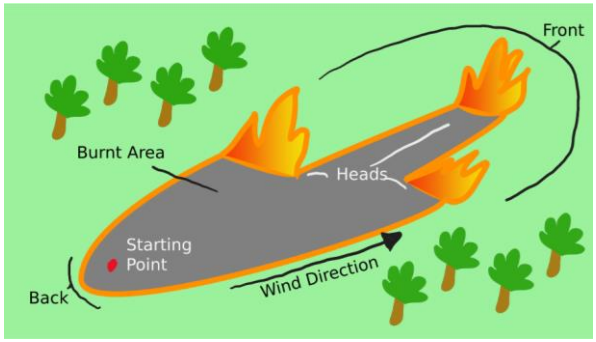

Figure 1: Schematic of a fire, inspired from Granström (2020, p. 7)

For wildfires to spread, variables such as drought and wind conditions need to be taken into consideration (SOU, 2019, p. 50). The illustration seen on the left, inspired from a report prepared by Granström (2020, p. 7) who followed the progression of the 2018 wildfires for the Swedish Civil Contingencies Agency (MSB), shows a simplified schematic of a fire (See Appendix D). Where a starting point can be seen, and with the wind direction playing a part in the direction of the spread of fire takes place. The area close to the starting point, against the wind direction, is called the back of the fire. If left untreated, a) the burning areas will run out of fuel or energy turning into burnt areas, and b) the fire will spread out following the direction of the wind in which active fires will be seen, which is called the front of the fire.

In the front, the heads can be seen with varying rates of spread from its starting point. Depending on the quality of the materials as sources of burning fuel and how tall the burning materials are, the spread could be in the range of two to three metres per minute, and in extreme cases from 15 to 30 metres to even 80 metres per minute (Granström, 2020, p. 12).

When thinking about a research topic to study in this master's thesis, I was interested in seeing the direct and indirect effects of humans on their surroundings. With climate change now being mainly caused by humans as per the IPCC (2007), and the encroachment of landscapes for society's varying needs, it is valuable to see what the outcomes are from such actions. As a fire spreads in the natural environment, there will be a point where it would interact with non-burnable objects such as roads in the geography. Since the presence of burnable materials in (paved and unpaved) roads are low, how much have the construction of the dense road and forest road network affected the spread of the fires, and in turn, burnt area?

The use of GIS or Geographical Information System has become a method and at the same time a science of its own, answering the question of "where" (Huisman and de By, 2009, pp. 26-28). By utilising the methods and technology of GIS, the study supplies a geographic aspect, and can highlight areas where the phenomenon of wildfires occurs the most, and see other variables that would affect the spread of wildfire in relation to the scientific problem

1.2 Scientific Problem

How do roads influence the size of a fire's burned area?

1.3 Aim of the study

The aim of this thesis project is to have a better understanding of how wildfires are affected in relation to the presence of roads acting as potential fire breaks. This is to see if there is a (positive or a negative) correlation between the spread of fires and their interaction with the road network. If we can observe any causation, planners can take steps to mitigate the wider spread of wildfires in the future. By understanding such tendencies better, strategies in road and roadside management, fire prevention and fighting can be improved.

This study could also be seen as an application of the methods learned throughout the master's programme in Geographic Information Sciences (LUMA-GIS) where a prevalent reliance of the methods and tools in GIS was needed to carry-out the study. As a culmination of these studies, the thesis project and this written report would somehow demonstrate the capabilities developed in the preparation, execution, analysis, and documentation of the project.

1.4 Limitations

As the events studied have occurred in 2018, there will be a heavy reliance on data that is already available. This means that the data could not be verified by doing field studies due to the temporality of the study, in addition to the logistical challenges of visiting all the sites. As mentioned in the SOU (2019) report, because more than two-thirds of fires occurred in a single weekend in July, only the meteorological data was considered for this month.

Given the number of fires that transpired in this time, the study did not seek further information on how the fires were eventually suppressed (whether done by air or land efforts), or if the fires extinguished themselves. Although suppression could greatly affect the overall outcome of a fire, the study aims to see if roads stand as a driver for the containment of fires. Though not included in the study, suppression efforts due to road access could serve as an added benefit from the presence of roads and not as a driver in itself. As an implication of this, it would be hard for the study to separate the abovementioned potential roles of roads, in addition to the co-variation of the increased presence of roads due bigger populations in potential firefighting.

1.5 Disposition

The study takes an exploratory approach, where several variables were tested to see if a specific variable could provide an insight on the interplay and interaction of fires and roads. In an effort to keep the manuscript succinct, the outcomes and variables seen throughout the study are only a fraction of what was examined and tested in the duration of the thesis course.

The succeeding chapter (Chapter 2) discusses the background of the study. It details what has happened in the 2018 wildfires in the country, as well as a theoretical overview of the different nuances of fires in relation to roads. The background chapter aims to supply a framework and justification as to why certain variables were used in the following chapters.

Chapter 3 discusses the methodologies, showing how the variables were treated and manipulated to proceed with the study. The chapter also goes through some of the transformations needed to conduct the analysis part and eventually in the presentation of the results.

The results chapter (Chapter 4) is divided into three sub-sections, and explains the results of two datasets that were created during the project. The chapter goes through a presentation of descriptive statistics to describe what has happened during the 2018 wildfires. This is then followed by a univariate regression (one-to-one) testing to justify the variables used in the multivariate regression where a model consisting of several predictive variables was created to answer the research questions. From the regression model, predictive maps were then created to highlight areas on their likelihood for bigger fires and the ratio of fire conformity with roads.

The fifth chapter, the discussion chapter, explains the results further, ultimately answering the research question set in the study. The chapter also aims to further justify the use and treatment of the variables to answer the questions.

The concluding chapter (Chapter 6) rounds off the study.

2 Background

2.1 Study Area

In the aftermath of the 2018 wildfires in Sweden, the government ordered an investigation from different government agencies such as: Swedish Government Official Reports (*Statens offentliga utredningar*) (SOU, 2019); The Swedish Civil Contingencies Agency (*Myndigheten för samhällsskydd och beredskap, MSB)* via Granström (2020); and the Swedish Transport Administration (*Trafikverket*) via Eriksson *et al.* (2018) to name a few.

Forest land covers 68% of Sweden's total land area, where circa 280 000 sq km. are classified as forest in Sweden's land area of 410 000 square kilometres (SOU, 2019, p. 33). Of the forest land, a significant part of this is industrial forest land at 235 000 sq km (p. 33). In a 2016 approximation by Statistics Sweden (as cited in SOU, 2019, p. 39), forestry-related activities contribute to Sweden's gross national product by 2.1 percent, or about 104 billion Swedish Kronor (Ekonomifakta, 2022). Forest land is important to the country as it not only provides industrial incentives, but also possesses environmental and cultural values to the people.

As the country started recording wildfire incidences in the 1800s, the 2018 fires could be counted as one of those spikes in the records such as what happened in 1903 and 1933 (SOU, 2019, p. 44). As detailed by Granström (2020, p. 19), wildfires started in the early part of the year in April, 2018. There was an increase in incidents in May and June, and another wave was seen in July, where most of the fires in terms of area occurred in a short span of days in the middle of July. The fire season ended in the middle of August, and in a few days the Swedish Government ordered for a full investigation and evaluation of what has happened during the 2018 wildfires (SOU, 2019, p. 3).

Using the dataset that was gathered for the study (Skogsstyrelsen, 2020), Table 1 shows the distribution of fires in terms of incidence and in the total fire area. Most of the fires that transpired during the year happened in Region Mitt in terms of incidence and total area of fires. By considering both Region Mitt and Region Nord, in terms of fire area, these regions make up more than 95% of the total fire area in 2018.

Table 1: Fire Incidence and Area per Region

Region*	Fire Incidence	Percent Incidence	Total Fire Area (km^2)	Percent of Fire Area
Nord (Norbotten, Västerbotten)	65	20%	18.12	7.93%
Mitt (Jämtland, Västernorrland, Dalarna, Gävleborg)	112	34.5%	201.67	88.21%
Väst (Värmland, Västra Götaland, Halland)	32	9.8%	4.64	2.03%
Öst (Uppsala, Västmanland, Örebro, Södermanland, Östergötland	53	16.3%	3.03	1.32%
Stockholm (and Gotland)	15	4.6%	0.13	0.06%
Syd (Jönköping, Kalmar, Kronoberg, Skåne, Blekinge)	46	14.2%	1.04	0.46%

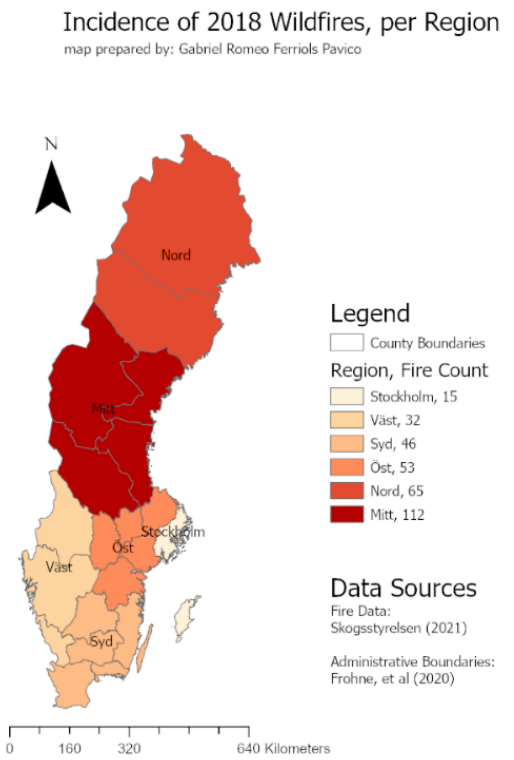

Figure 3: Incidence of 2018 Wildfires

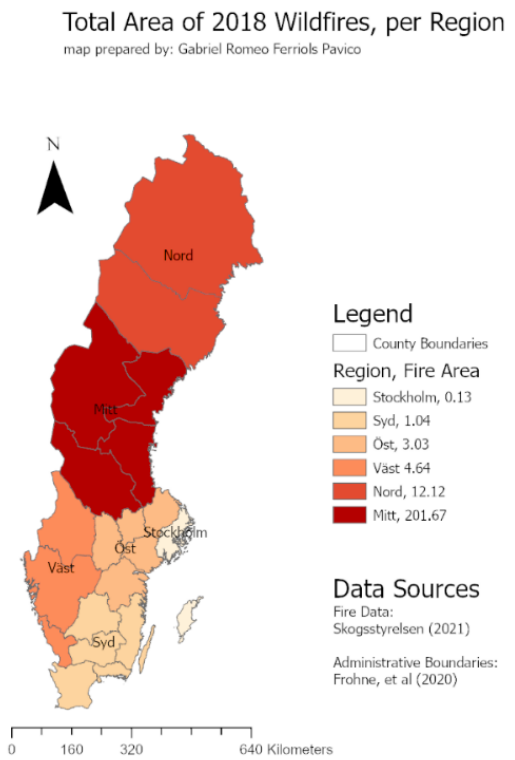

Figure 2: Total Area of 2018 Wildfires

*The counties were grouped together according to the Swedish Transport Administration's road dataset, which will be discussed later in the method chapter. Above is a visual representation of Table 1 in map form.

Granström (2020, p. 3) discusses how several indices pertaining to fires, one of which is the Fire Weather Index (abbreviated as FWI, an index used to predict the intensity and spread of fires when ignited), was constantly high that made the country vulnerable to fires. In addition to this, there were instances of warm moist air which caused heat thunderstorms, causing some of the fires during that time (SOU, 2019, pp. 28-29). With periods of constant and heightened fire risk, this caused Sweden to experience a fire season that was ten times larger than its usual annual occurrence of fires (SOU, 2019, pp. 49-50). This is the main reason for focusing the study on the 2018 data as the rate of fires are exaggerated, and there are more data to be able to test and answer the questions.

There were efforts in supressing the fire both on air and on the ground. What was seen in the MSB report (Granström, 2020, pp. 4, 144) was that planes were effective in supressing the fires in 'broader strokes', however, suppression efforts by land were still necessary to stifle the remaining embers in these sites. This was also in accordance to the other investigation submitted to the Government (SOU, 2019, pp. 19, 225) where it was seen that the procedures after suppression (*eftersläckning*) needed to be reformed, as fires tended to reignite from the embers once the weather becomes ideal again for propagating these fires. To add to this, route data was not easily available for the air suppression efforts, making it hard to conduct evaluations how fires were actually managed (Granström, 2020, p. 149). This is why suppression efforts were not looked at for the study.

In a report by the state-owned broadcaster, SVT, it was estimated that the insurance payout for damages to the forestry industry amounted to 800 million SEK (Vikström, 2018). There are more damages to this wildfire event as a report by the Swedish Transport Administration saw that 420 kilometres of roads were damaged, costing about 6 million SEK (Eriksson *et al.*, 2018). Aside from the damages on property, the wildfires release carbon dioxide back to the atmosphere, which adds more burden to the world's efforts against climate change.

From this point on, we will go through related literature on different wildfire studies.

2.2 Fires, roads, and landscapes

A study on African Savannah fires by Takacs, Schulte to Bühne and Pettorelli (2021) used meteorological factors and landcover in its influence in the area or spread of the fires. They saw that the type of vegetation seen in the different landcovers played a role in the spread of fires. And in this case, the presence of grass and shrubbery, drove larger areas of fires compared to forests that spread slowly. When fires ignite further from roads, these tended to spread faster than those igniting closer to roads that act as fire breaks.

In a study on fire incidences in Terai, North-eastern India, a region that is predominantly grasslands and savanna-woodlands, Banerjee, Das and John (2021) found that along with meteorological factors, variations in land cover played a role in the incidence (i.e. frequency) of fires when plotted in a grid. When the researchers compared between grass, forest and woodlands, it was discovered that grasslands recorded more fires given the context of the area. This is due to the region's cultural and historical practices as a number of these fires were started by humans to control the encroachment of trees into grasslands. As a result of these practices, human-caused wildfires occur closer to roads, giving a negative correlation of fire incidence to road distance.

Narayanaraj and Wimberly (2012), on a study in the Cascade Mountains in Washington State, USA, found that anthropogenic causes of fire can be seen closer to roads and in areas of high road densities. Furthermore, fires, regardless of how they were ignited, tended to become larger in remote areas. Given the remoteness of fires, the researchers hypothesised that detection would be harder until the fires have reached their tipping point in its visibility. The researchers also hypothesised that given the lack of paved and gravel roads in the wilderness, the unfragmented landscape, has caused wildfires to become bigger.

In the same study, there is a duality that can be seen in the effects of the roads. They also noted that the edges of landscape as a result of road creation caused certain microclimates in these areas, making it also susceptible to fire spread. Molina *et al.* (2019), in a study of roadside ecology in Spain, somehow agrees to this where they also found that roadsides can be preferable habitats to certain vegetations, which in turn have varying susceptibility to ignition, given their interplay with external elements. In a separate study, Narayanaraj and Wimberly (2013) add more nuance to their 2012 fire research, wherein they found out that fires tend to

be less severe (i.e. vegetation mortality) in zones closer to roads, given the difference in the makeup of potential fuel for forest fires compared to zones farther from the roads.

The number of studies regarding the interplay of roads and landscapes in relation to wildfires has been limited in the Swedish context, as also discussed by Pinto *et al.* (2020). Focusing on the fire seasons from 1998 to 2017, the researchers found that the occurrence of fires was higher in areas of high road and population density but given the presence of fuel breaks and heightened visibility of fires, these did not translate to larger fire areas. The group found that the amount of road density, together with forests, respectively provide a negative and positive relationship to fire sizes. They also stressed on the fact that meteorological indices also played a factor in fire sizes.

2.3 Fire and road density

From the Swedish study and by the other studies, there has been a distinction between the frequency and the sizes of the fires (Pinto *et al.*, 2020; Narayanaraj and Wimberly, 2012). These claims are also in congruence with the review by Forman and Alexander (1998, p. 223) where they discussed how road density in the natural landscape has led to the increase of incidences of fire, while at the same time negatively affected the sizes of the fires either as fire breaks or access roads for fire suppression. The inverse of this effect is a study conducted by Leonard, Plantinga and Wibbenmeyer (2021) where in the United States, fires tend to be bigger in areas that are inaccessible to roads. The inaccessibility of these areas via roads would become a hindrance in fire suppression efforts, and it would be harder for forest managers to enact preventive measures to minimise the available fuel in forested areas that are inaccessible.

Sjöström and Granström (2020), as cited by Granström (2020) for the Swedish Civil Contingencies Agency, mentioned that the placement of rescue services in relation to the road networks in the country should ideally allow firefighters to reach fires within 25 minutes. Efforts via helicopters would be helpful, but still land efforts are essential as detailed in the several government reports. The direct and indirect influence of humans can be seen all throughout the process of fires: from the possible ignition to the detection, to carrying out the suppression effort, plus the existence of roads – humans have a hand in this.

2.4 Fire perimeter conformity

In a study conducted by Yocom *et al.* (2019) on the wildfires that occurred in forest situated in Arizona and New Mexico, USA, they explored the concept of conformity where the edges (i.e., the perimeter) of fires would follow the contours of roads and previously burnt areas from older fires acting as fuel breaks. What was seen in the study was that fires had an average road conformity of 25% of the perimeter, and against older fires at 8.7 percent. When the time gap between two fires is sufficiently long for new production of fuel, the study found that there is a tendency that the new fire could encroach the area of a previous fire. This implies that newer vegetation found in the previous fires would have been able to serve as burnable material to enable the wildfires to spread further in previously burned areas. Conversely, when the older wildfire is within 5 years of the studied wildfire, the perimeter of the newer wildfire would conform to the edges of the older wildfire. This study indicates the significance of burnable materials (or the lack thereof) in how wildfires spread and take shape. This study however did not look deeper at the effects of fire sizes with their degree of conformity with the said fire breaks.

2.5 Fire and population clusters

In the question of human inhabitation, Pinto *et al.* (2020) used population density as a driver for fire occurrence. As discussed earlier, the closer the fires are located to man-made structures are, in-effect more visible for notifying the authorities. This is exactly the case in Patagonia, Argentina (Mundo *et al.*, 2013), where the fire ignitions were more frequent close to towns, having a negative relationship between the two variables. The same tendency is seen in a study on human-caused wildfires on Vancouver Island in Canada (Pew and Larsen, 2001) even when the study area was divided into grid cells. As data was analysed per grid cell in the Canadian study, mean values were looked at instead of total values. As an example, they were looking at mean fire sizes as a predicted variable in their study.

2.6 Fire Weather Index

The Canadian Forest Fire Weather Index, or commonly called as FWI, pertains to a risk level of an area has in the occurrence and spread of the fire. This is comprised of several meteorological observations, resulting into different sub-indices, eventually producing an FWI. Figure 4 as seen below are the schematics of the FWI inspired by Lawson and Armitag (2008, p. 2):

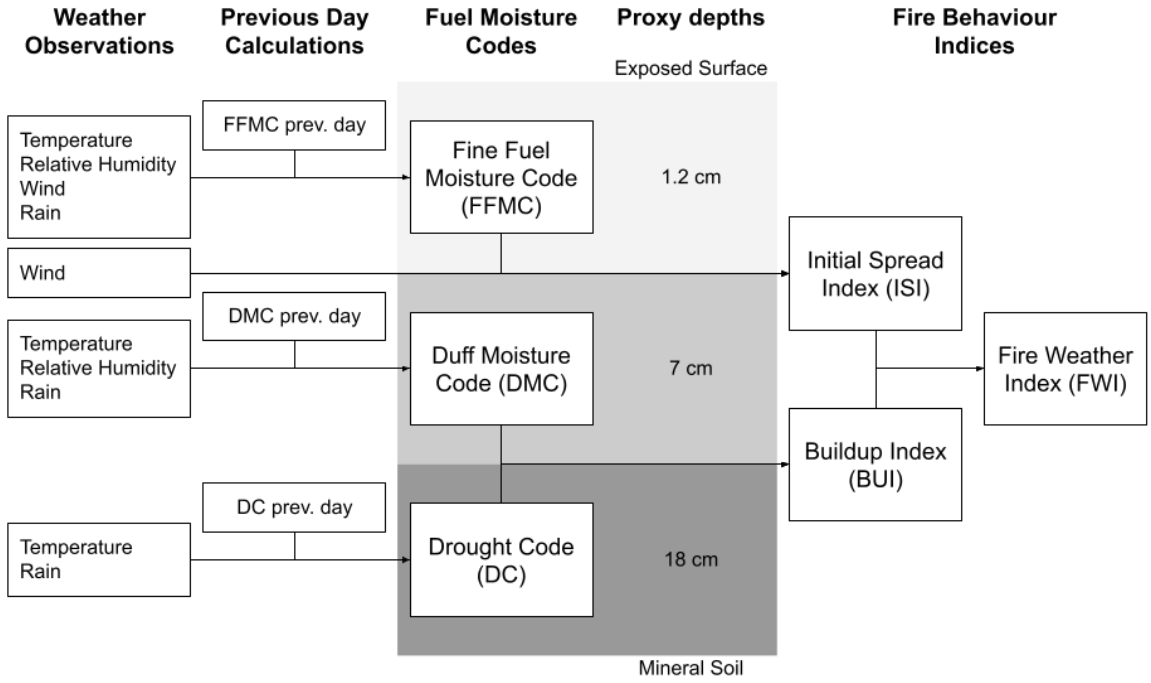

Figure 4: Fire Weather Index schematics, inspired by Lawson and Armitag (2008, p. 2)

The Fire Fuel Moisture Code (FFMC) is comprised of observations such as temperature, relative humidity, wind and rain, plus the same value from the previous observation day. These variables stand as a proxy calculation to determine "the ease of ignition and flammability of fine fuels" (Lawson and Armitag, 2008, p. 2), i.e. material that is about 1.2 centimetres from the top of the forest floor layer (p. 3). From the FMMC and wind, the Initial Spread Index is derived. The ISI indicates how fast the fire would spread should there be an ignition event.

The Duff Moisture Code (DMC), which considers the moisture of the duff layer that is about 7 centimetres from the exposed surface, is comprised of observations of temperature, relative humidity and rain along with the DMC value for the previous day. The Drought Code (DC), only comprised of temperature and precipitation, and the previous day's DC value, indicates the moisture (or the lack thereof) of compacted organic layer, about 18 cm from the top of the

exposed forest surface. Both DMC and DC make up the Build-up Index (BUI), which estimates the amount of available fuel if ignition happens. After deriving the ISI and BUI, the Fire Weather Index is then produced, providing an estimation of intensity of fires if and when they happen. The FWI is easier to derive as it is only comprised of the four measurable meteorological elements which can be used for historical analysis of fire trends.

Though it originated in Canada, FWI is used even in Europe and in Sweden for analysing and predicting areas that would be affected dramatically when ignition events happen (Vitolo *et al.*, 2019; Krikken *et al.*, 2021). Although Sweden's FWI values are relatively low when compared to those for Southern Europe as what was seen in Vitolo *et al.* (2019, p. 26), the fire events still caused damage to the entire value chain of industries, property, public safety and the environment.

In a separate study conducted by Krikken *et al.* (2021) on the Swedish wildfires of 2018, by using FWI as an explanatory variable to the fire incidents, they found that FWI alone does not explain the events that transpired for the year. Human behaviour, forest management and the ecology of the landscapes are additional variables that could explain the variation in fires for that time period. Although evaluated as a good predictor in the Swedish context, FWI only gives a fraction of the prediction without looking at the composition of geography of the affected areas (Pagnon Eriksson and Johansson, 2020, p. 12). The country's FWI in July 2018 was constantly high when compared to Sweden's previously recorded values in previous years as stated by Granström (2020), and corroborated by Krikken *et al.* (2021), which explains low variation of this metric. This, in turn, could be an explanation why the events are not effectively explained by this index. The group of Krikken *et al.* (2021) continues that although FWI is still a good indicator, temperature as an added independent variable could be considered to be driver to fire risk.

Similar behaviours of FWI were also seen in another master's thesis from the Department of Physical Geography and Ecosystem Science in Lund University (Gomes, 2022), where there was no linear progression of Fire Area in Portugal (1980-2019) against FWI (among other variables). Gomes observed that mid-range FW indices incurred larger fire areas than that of 'very high' and 'extreme' indices. This is also the case for a study in France where "fire frequency and burned area do not entirely reflect FWI patterns" (Fox *et al.*, 2018, p. 126), as the study saw that the linear relationships between FWI and frequency and burned area are only true up to a certain FWI threshold of 90 (p. 129).

2.7 Moving forward

From this overview of related literature, there are some key takeaway messages:

Fires are dependent on the quality of the materials with the potential to burn. This means that the type of landcover is essential when studying fires. Based on the earlier subsection, Sweden consists of sixty-eight percent forest land, and a huge part of it is used for forestry.

Fires start either by natural or anthropogenic causes. More fires happen closer to man-made features such as towns and roads due to human activities in the area and, in some cases, the types of vegetation that thrives close to roads. In turn, identification and notification of fires could be processed quicker than areas away from these structures. The roads come with different uses, where they stand as an access channel for fire management vehicles to be situated close to the fires. Roads also stand as a fire break as they cut the continuous landscape for fires to spread. Roads can therefore both increase and decrease burnt area, and it remains unclear how and why they affect the amount of burnt area in Sweden.

The farther the fires are from these man-made features, the more there is a tendency for them to become larger. Given that fires would be farther away, identification and notification would be delayed until the fires become big (producing more smoke) to become noticeable. Moreover, with little interaction with roads serving as fire breaks, fires tend to become larger given the bigger parcels of continuous landscapes.

Meteorological indices such as FWI, could explain some of the behaviours of the fires, but fire events do not operate in the vacuum of meteorological observations alone. As predicated in Chapter 1, the potential of the land cover as a fuel is an important factor that is neglected by FWI. Moreover, FWI does not consider human behaviour in terms of ignition, and to an extent, the efficiency or inefficiency of suppression of the fires. And in this study, built surfaces such as roads could interplay with FWI in deciding how the fires would eventually look in the end.

The study will consider these takeaway messages and apply them in the methods section.

3 Methodology

3.1 Datasets

Table 2 outlines the different datasets used in the study.

Table 2: Overview of the different datasets in the study

Short Name	Retrieved Name	Projected Coordinate System	File Information	Data Source	Description
Sweden Boundaries	geoBoundaries_ SWE_ADM1	WGS 1984	Polygon Shapefile	geoBoundaries, see Frohne *et al.* (2020)	A Polygon covering the different county boundaries of Sweden.
Fires	brand	SWEREF99 TM	Polygon Shapefile	Skogsstyrelsen (2020)	A polygon shapefile covering the different fire extents in Sweden for the year 2018 to 2021.
Roads	main.TNE_FT_ Vaghallare	SWEREF99 TM	Filetype SQLite Database Polyline Sourced Regions Nord, Mitt, Väst, Öst, Stockholm, Syd	Trafikverket (2022)	Road Network of the different regions in Sweden for emergency services.
Land Cover	my_riks	SWEREF99 TM	Polygon Shapefile	Lantmäteriet (2021)	A tiled polygon layer detailing the different land covers in Sweden.
Fire Risk Points	Brandriskvärden juni-juli 2018	SWEREF99 TM	Microsoft Excel File	Myndigheten för samhällsskydd och beredskap (2022)	An excel file detailing the observed meteorological values in the different weather stations in Sweden, per day from June to July 2018.

3.2 Geoprocessing

The Geographic Information System program ArcGIS Pro (version 2.7.3) was used to carry out the various geoprocessing of the different datasets. All files were then reprojected in SWEREF99 TM projection. Below is a visual representation of the different steps executed from the originating files in 3.1, creating derivative data for the study. These processes will be discussed in the succeeding subsections. To avoid intersecting lines in the flowchart, connecting objects represented by letters A to D enclosed in circles are used to link one object to the other depending on the direction of the arrow. Rhomboids signify input and output data files, while rectangles signify the various geoprocesses.

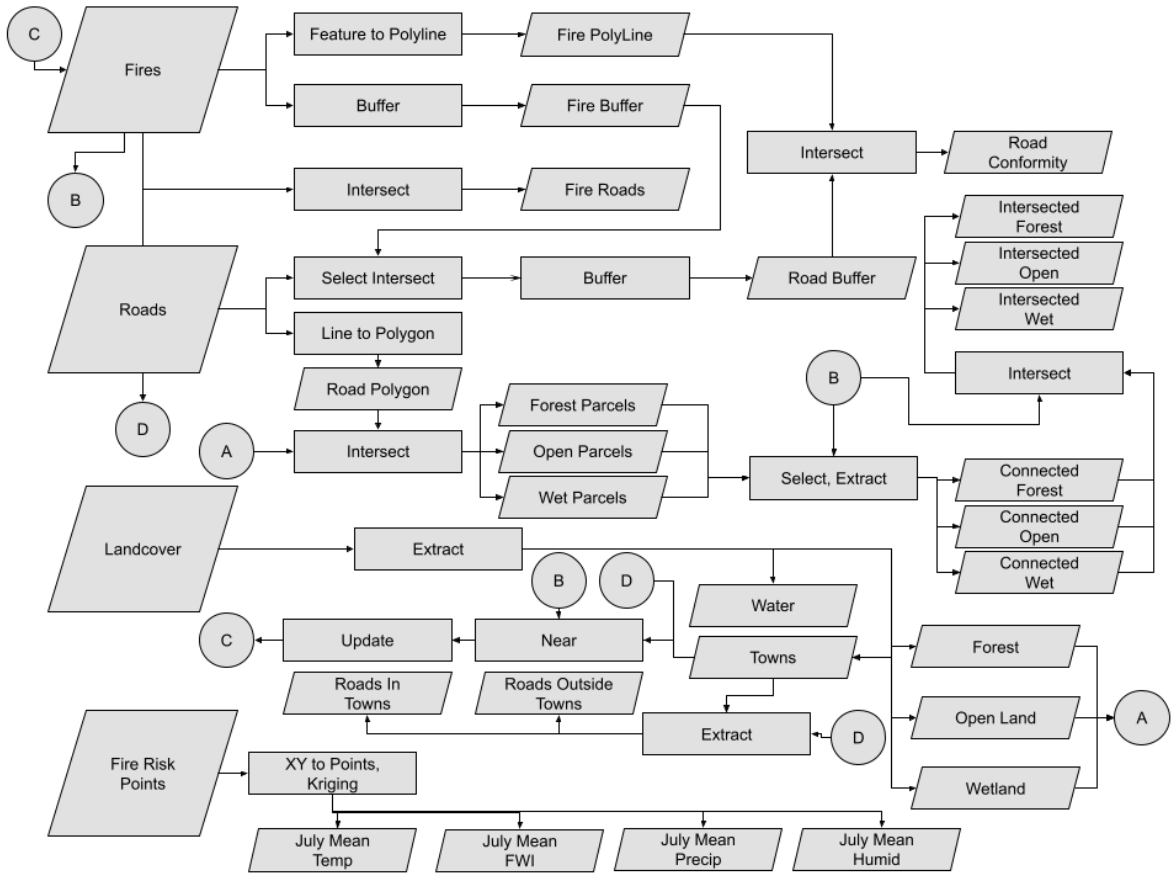

Figure 5: Flowchart of Geoprocessing in this study

The following subsection (3.2.1 to 3.2.4) describes the process in greater detail. To give an overview of the processes, it can be summarised to three general themes.

For fires, the idea is to utilise the roads to extract the lengths that intersect with fire polygons and to extract the length of the fire perimeters that conform with roads. For fires that did not interact with fires, the distance is taken to its nearest road.

For landcover, these are divided into smaller parcels of land if a length of road cuts through these layers. Differentiations are created between landcover types, and identifying the parcels of land that were burnt when intersecting with the fire polygon. Roads are also differentiated if they fall within the confines of a town or outside of it. The distance between fires and the nearest towns were also taken for analysis.

Meteorological observations were taken into consideration for the succeeding statistical analyses.

3.2.1 Fires

The fire data is sourced from the Swedish Forest Agency (Skogsstyrelsen). In the dataset, only fire features that were observed in 2018 were selected for the study. The resulting selection included 325 individual features. These features were then inspected individually to see if there had been errors in the digitisation of the data. One fire was edited as some suspected erroneous polygons were included in the feature that were far from the main fire site.

There are no specific dates listed in the attribute table of the shapefile, but it is assumed to have happened in the month of July, as mentioned in the report of SOU (2019) where the majority of the fires, in terms of the burned area, happened in this month.

The geoprocessing tool ‘feature to polyline’ was used to turn the perimeter of the individual fires as polylines. *New derived data: fire_polyline*

A buffer of 1 kilometre per fire feature was created to be used a selector layer in the succeeding geoprocessing operations. *New derived data: fire_buffer*

3.2.2 Roads

The dataset from the Swedish Transport Administration (Trafikverket) was packaged as a divided layer file, grouped per region in Sweden: North (Nord), Mid (Mitt), West (Väst), East (Öst), Stockholm (and Gotland), and South (Syd).

The roads were intersected with the *fire* layer to extract only the line segments within the burnt forest areas. Object IDs were retained to be able to join the tables for the statistical analysis. *New derived data: fire_roads*

The line feature of roads was transformed into a polygon file where enclosed lines would result in a closed polygon. The resulting polygon was then selected from the spatial relationship with the fire buffer, and features not intersecting with the buffer were then deleted. However, as the road files were divided into the different regions, areas between regions did not yield closed polygons. Manual corrections were made to create enclosed polygons that would intersect with fire buffers located in these gaps. *New derived data: road_polygon*

Using the 'near' geoprocessing tool, the fire perimeter was measured with respect to its proximity to the nearest road feature. Features that have intersecting fire roads would result to zero. *Updated attribute table: fires$road_dist*

The idea to extract road segments acting as fire borders, as well as the method on how to find these segments, were inspired by Yocom *et al.* (2019) when looking at conformity of fire perimeter with roads and previously burned areas. In the case of this thesis project, only *roads* intersecting with *fire_buffer* were selected for computational efficiency. The selected roads were then processed further to create a 30-metre buffer for each side of the line feature. The buffer size is smaller when compared to the study by Yocom *et al.* (2019), where 60 metres of buffer was created for each side of the road. *New derived data: road_buffer*

The *road_buffer* was then intersected with the converted polyline feature *fire_polyline* of the fire perimeter to derive the fire perimeter conforming to the roads. *New derived data: road_conformity*

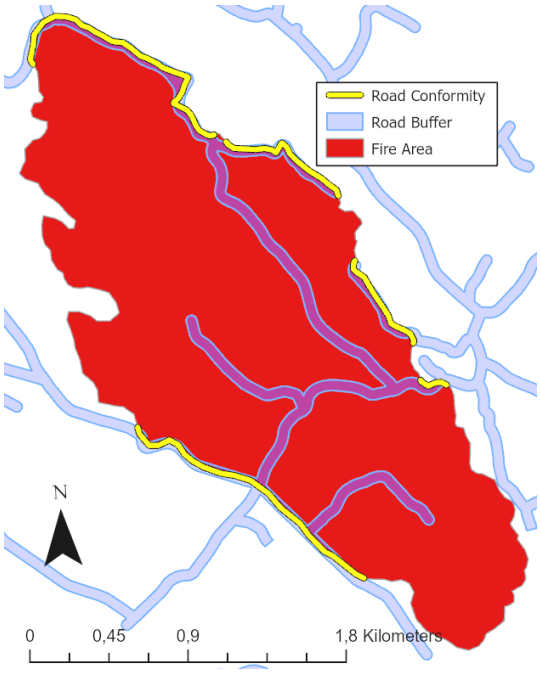

Figure 6: Schematic of Fire Conformity (Fire ID 134)

This is a screenshot of a fire located in Västernorrland county in red, with road_buffer in translucent blue, and the conforming fire perimeters inside the buffered zones in yellow.

3.2.3 Landcover

Basing on the Swedish Land Survey Authority's (Lantmäteriet) documentation for this dataset, landcover features with the KKOD classification of 901 (water), 302 and 303 (towns), 601 (forest), 611 (open landscapes), and 911 (wetland) were selected and exported to create the different layer features.

As the original landcover data was divided in tiles, the data was then merged according to classification, and eventually 'exploded' to separate features with matching attributes that are not adjacent to each other. The derived forest, open and wetland were then exported as a copy for further editing. *New derived data: water, towns, forest, open, & wet*

Using the near geoprocessing tool, the *fire* sites were measured to its nearest *town* features. *Updated attribute table: fires$town_dist*

To be able to produce the parcels of landcover (*forest, open* and *wet*), each landcover feature was intersected with *road_polygon* to cut the features into smaller polygons representing continuous land covers. *New derived data: forest_parcel, open_parcel, & wet_parcel*

The newly created parcels of landcover were selected if they intersect with the fires. The selection was then extracted to new feature layers. *New derived data: connected_forest, connected_open & connected_wet*

The connected landscapes were then intersected against the fire polygon to extract the type of

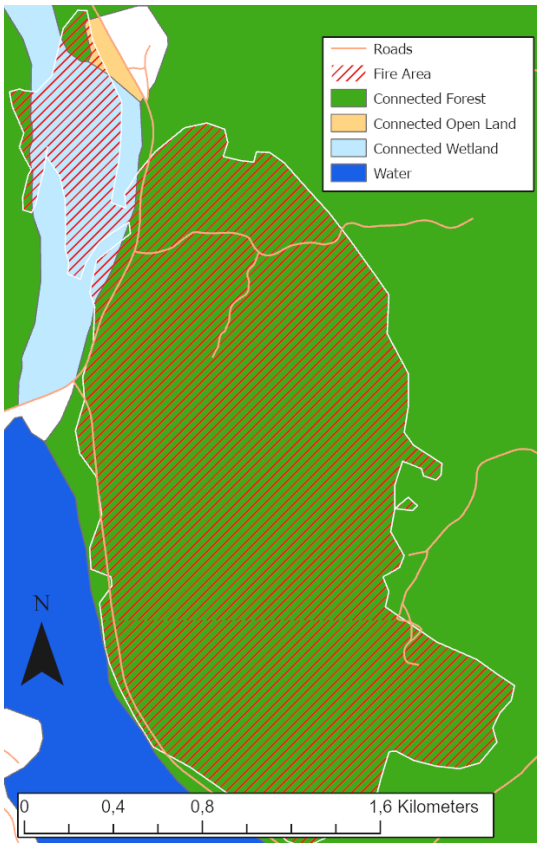

Figure 7: Schematic of Connected and Intersected Landcovers (Fire ID 61)

This is a screenshot of a fire located in Jämtland. The perimeter of the fire displayed in white outline, with the intersecting areas seen in red hatched lines against the landcovers of forest (green), wetlands (light blue), and open land (light brown). Roads are shown (in salmon pink) to show how the connected areas are cut out against the road lines as seen in the case of the open land seen in the north and the wetland seen in the west of the fire area.

landcover that was burned. *New derived data: intersected_forest, intersected_open & intersected_wet*

To be able to differentiate the roads inside and outside of towns, *roads* were split using the *town* feature. *New derived data: roads_in_towns & roads_outside_towns*

3.2.4 Fire Risk Points

The dataset received from the Swedish Civil Contingencies Agency contains meteorological data recorded in 7 892 stations across the country, covering daily observations of the months of June and July. The file included values such as precipitation, temperature, FWI, windspeed, and relative humidity. The data was organised to classify data according to the calendar month. The mean values for temperature and FWI for July were selected and transferred to ArcGIS as a point layer. The points were then interpolated, with a raster resolution of 1 km. See Appendix A – Python Scripts, Script 1: Weather Kriging. *New derived data: July_mean_temp, July_mean_FWI, July_mean_precip, & July_mean_humid*.

3.3 Data Tabulation

There will be two ways of tabulating the data and performing the data analysis: per fire site and per grid analysis.

3.3.1 Site Dataset

Using the Fire ID as a way to join data, the following variables were tabulated together:

Table 3: Tabulated Per Site Data

Tabulated Data (Per Site)	**Derivative Layer / Feature**
Fire Area (km^2)	*fire*
Fire Perimeter (km)	*fire*
Fire Road Length (km)	*fire_road*
Fire Road Density (km/km^2)	*fire_road* ÷ *Fire Area*
Road Conformity Length (km)	*road_conformity*
Road Conformity Percent	*road_conformity* ÷ Fire Perimeter
Distance to Roads (km)	*fire*
Distance to Towns (km)	*fire*
Intersected Forest Area (km^2)	*intersected_forest*
Intersected Forest Percent	*intersected_forest* ÷ Fire Area
Intersected Open Land Area (km^2)	*intersected_open*
Intersected Open Land Percent	*intersected_open* ÷ Fire Area
Intersected Wetland Area (km^2)	*intersected_wet*
Intersected Wetland Percent	*intersected_wet* ÷ Fire Area
Connected Forest Area (km^2)	*connected_forest*
Connected Open Land Area (km^2)	*connected_open*
Connected Wetland Area (km^2)	*connected_wet*

3.3.2 Grid Data

For the grid dataset, a fishnet grid was created over the extents of the administrative boundaries of Sweden. A motivation to use this method is to be able to look at other variables that are available in a grid, that could possibly explain the variation seen in fire behaviour. As what will be discussed later, there are fewer, but larger, fires that overrepresent the total burnt area for the year. By looking at mean areas in a grid, this can help normalise the distribution of the data. Each cell has its own unique object ID, and the resolution for this is 10 000 square kilometres (100 x 100 km). To tabulate the vector data, the features were split where they intersected the grid lines. The resulting polygons were then tabulated via the geoprocessing tool 'Summarize Within' for the totals, and a python script to get the mean values per grid. See Appendix A – Python Scripts, Script 2: Mean and Median Values for Grid Polygons.

For raster data of temperature and FWI, 'Zonal Statistics as Table' via arcpy was used to get the mean value for the different variables. See Appendix A – Python Scripts, Script 3: Zonal Statistics for Rasters and Excel Conversion. The variables were then manually consolidated based on the Grid ID. Below are the variables that was used and analysed for the grid dataset.

Table 4: Tabulated Grid Data

Tabulated Data (Per Site)	**Derivative Layer / Feature**
Sweden Land Area (km^2)	*Sweden Boundaries*
Fire Area (km^2)	Sum(*fire*)
Mean Fire Area (km^2)	Mean(*fire*)
Fire Perimeter (km)	Sum(*fire*)
Fire Incidence	Count(*fire*)
Mean Distance to Town (km)	Mean(*fire$fire_dist*)
Road Conformity Length (km)	Sum(*road_conformity*)
Road Conformity Percent	*Road Conformity Length ÷ Fire Perimeter*
Road Density Outside Towns (km/km^2)	Sum(*roads_outside_towns*) ÷ (*Sweden Land Area* – Sum(*towns*))
Forest Mean Area (km^2)	Mean(*forest_parcels*)
Open Land Mean Area (km^2)	Mean(*open_parcels*)
Wetland Mean Area (km^2)	Mean(*wet_parcels*)
Mean Temperature (°C)	Mean(*July_mean_temp*)
Mean FWI	Mean(*July_mean_FWI*)

3.4 Statistical Analyses

After tabulating the data, the values were then transferred to SPSS version 28 for statistical analysis. Descriptive Statistics were used to detail what has happened in the 2018 wildfires. Upon seeing that the fire sizes and other variables were not normally distributed, a logarithmic transformation of base log was applied to normalise the distribution. See Appendix B – Statistical Tables.

Using the transformed data, univariate and multiple regression was conducted using the following dependent variables:

- Fire Area (km^2)
- Fire Road Conformity (%)

Additional scatter plots, as seen in the univariate analysis were created in Python, via Matplotlib and Seaborn (Hunter, 2007; Waskom, 2021). Partial regression plots were created using statsmodels (Seabold and Perktold, 2010) that are seen in the multivariate regression analysis.

From the results of the multiple regression, a map was constructed to visualise the regressed model using the following equation:

$$Risk = x_i \cdot \beta_i \cdot R_i^2 + x_{i+1} \cdot \beta_{i+1} \cdot R_{i+1}^2 + \ldots + x_k \cdot \beta_k \cdot R_k^2$$

Equation 1: Consolidation of x in model

The equation fits the results of the regression model that would eventually highlight the likelihood of the two dependent variables, as: a) the areas that would risk having higher mean fire areas in the country, and b) areas that would have the likelihood for relative road conformity. The significance and meaning of this equation will be further illustrated in the Results chapter below.

4 Results

The results presented in this chapter are divided into three sections using different statistical methods such as: descriptive statistics (4.1), univariate regression (4.2), and multiple regression (4.3).

Two datasets were created and analysed in this chapter, stemming from the methods described in the previous chapter. The first is the individual fire site dataset and the second is the grid dataset. These datasets will help create a narrative of the dynamics of the 2018 fires in Sweden, and eventually answer the research question for this study:

- How do roads influence the size of a fire's burned area?

Some discussion will also be included in this chapter to summarise the results and provide motivation on how the data was treated and presented.

4.1 Descriptive Statistics

4.1.1 Fire Sites

There were 325 individual fire sites recorded by the Swedish Forest Agency (Skogsstyrelsen) and the Swedish Civil Contingencies Agency (MSB) from the year 2018. Although the sizes of the fires are not normally distributed, these figures describe the fires and how the ignition events transpired. Please see Appendix B, Test of Normality: Fire Areas, Per Site. As mentioned in the Methods chapter, the figures were corrected by applying natural logarithm, and will be used starting from section 4.2.

Table 5: Summary of 2018 Wildfires, Per Site

	Min	**Max**	**Sum**	**Mean**
Fire Area (km^2)	0.0006	43.26	228.65	0.70
Fire Perimeter (km)	0.09	92.74	761.39	2.34

The country incurred a burnt area of 228.65 square kilometres from the 325 fire sites. This figure is in line with the estimates in the report to the Swedish government on the 2018 wildfires (SOU, 2019, p. 109). In terms of range, the smallest fire area amounted to 557 square metres

(0.000557 km^2), while the largest area resulted to 43.26 square kilometres. The fire sizes averaged at 7/10 of a square kilometre (0.70 km^2).

As a fire's area spreads, the perimeter of the fire becomes longer. The fire perimeter amounted to 761 kilometres, with the shortest perimeter of a fire recorded as 86 metres and the longest with 92.74 kilometres. The average length of the perimeter computed as 2.34 kilometres per fire site.

Of the fire sites, Table 6 below shows that 22% (73 sites) intersected with roads, with a total of 336 kilometres of roads being affected. Even though it was only 22% of the fires, these seventy-three fires that intersected with roads contributed to at least 93% of the total fire area during the 2018 wildfires.

Table 6: Intersected Roads

	N	**Min**	**Max**	**Sum**	**Mean**
Fire Area (km^2)	73	0.001	43.26	213.65	2.93
Fire Perimeter (km)	73	0.18	92.74	549.56	7.53
Fire Road Length (km)	73	0.0003	89.85	336.05	4.60
Fire Road Density (km/km^2)	73	0.03	38.42	-	4.38

The length of these intersected roads is in line with the report to the Swedish Transport Administration (Trafikverket), wherein 420 km of road was repaired after due to the 2018 wildfires (Eriksson *et al.*, 2018, p. 17). The 336 kilometres of roads do not include the surrounding roads close to fires, which will be discussed in Table 7.

Road density can be derived from the length of the intersected roads per area of the individual fire. Of the 73 sites intersecting fires, the mean density is 4.37 km/km^2, which is relatively close to the average intersected road length of 4.6 kilometres.

Revisiting the methods section, road conformity is derived from buffered areas of the road line layer, with thirty metres buffer on both sides of a given road segment. Converting the fire polygons as line features to only detail the perimeter of the fires, these were intersected against the buffered areas from the roads.

Table 7 shows that there are 116 fire sites that "conformed" some of their perimeters with the buffered road areas. This can be compared with Table 6, where only 73 fire sites intersected with roads. In this case, these 116 fire sites, conformed to various degrees with roads represent

95% of the total burnt area for 2018. When inspecting the dataset, all fires that have intersected with fires also have varying lengths of their perimeter conforming to roads.

Table 7: Road Conformity, Distance to Roads and Towns

	N	Min	Max	Sum	Mean
Fire Area (km^2)	116	0.0009	43.26	217.09	1.87
Fire Perimeter (km)	116	0.11	92.74	593.48	5.12
Road Conformity Length (km)	116	0.02	25.27	109.24	0.94
Road Conformity Percent	116	0.67	90.5	-	26.79
Distance to Towns (km)	325	0.00	43.43	-	7.78

109 kilometres of the fires' perimeter conformed with the buffered road areas. By chance, this length corresponds to 14% of the total fire perimeter incurred in the 325 fire sites.

Relating to the results in Table 6, the 109 kilometres of fire perimeter conformity to roads, adding to the 336 kilometres of intersected roads within fire sites can address to the report of the Swedish Transport Agency of 420 kilometres of road needing repairs due to the fire events (Eriksson *et al.*, 2018).

Of the 116 sites conforming their perimeters to roads, the smallest relative conformity, or percentage, was seen to be at 0.67% or 38 metres, having a total length of 5.7 kilometres for a particular fire site. The highest percentage of road conformity was observed to be at 90.50%, or 0.26 kilometres of the perimeter conformed out of 0.29 kilometres of the fire perimeter in a particular fire site. The average conformity percent was seen to be at 26.79% for all 116 sites.

There is one fire that occurred inside the confines of a town in Stockholm County, which explains the minimum distance to zero in the descriptive statistics for this variable. While the average distance to the towns is 7.78 kilometres, the maximum distance to a town for fires is more than forty-three kilometres.

By selecting the fires that had **not** conformed their perimeter to roads, i.e., the inverse of Table 7, the area only corresponds to five percent of the total burnt area for the year as shown in Table 8. The average size of the 209 fire sites was seen to be at 0.06 square kilometres. The distance of the selected fires to the nearest roads was seen to be ranging from 0.03 to 2.15 kilometres, with an average distance of 0.29 kilometres.

Table 8: Fires with no Road Conformity

	N	Min	Max	Sum	Mean
Fire Area (km^2)	209	.0006	1.74	11.55	.06
Distance to Roads (km)	209	.03	2.15	-	.29

It must be noted that there were four fire sites that had an area that was greater than 10 square kilometres, totalling to 155.13 km^2. When not considering these larger sites, the total burnt area is 73.51 km^2, where sites that interact with roads account for 84%, while those that do not account for 16% of the burnt area.

The table below describes the burned landcovers during the wildfires of 2018. 314 of 325 fires intersected with forest areas. The area of burnt forest corresponds to 88% of the total burnt area. Of the 314 fires, the average percentage of burnt forest can be seen at 95%.

26.49 square kilometres of wetlands were burnt, amounting to 11.58% of the total fire area. 55 sites intersected with wetlands, and the average intersection can be seen at 40%.

Only 0.125% or 0.29 square kilometres of the total burnt area can be attributed to open landscapes. 17 of the 325 sites intersected with open landscapes. Moreover, the average intersection recorded in open landscapes can be seen at 11%.

Table 9: Burnt Landcover

	Min	Max	Sum	Mean
Intersected Forest Area (km^2)	0.00004	42.06	200.87	0.64
Intersected Forest Percent	1.47	100	-	95.25
Intersected Open Land Area (km^2)	0.00004	0.20	0.29	0.02
Intersected Open Land Percent	0.01	100	-	10.71
Intersected Wetland Area (km^2)	0.002	9.50	26.49	0.48
Intersected Wetland Percent	0.95	100	-	39.93

4.1.2 Grid dataset

71 grid cells of 10 000 km^2 cover the extent of Sweden, with some covering the country fully, and some partially. Of the 71 cells, 24 cells had no record of fires in the area. The highest incidence of fires (as seen in Figure 8) in one grid cell was observed to be at 25 incidents, and

325 fire sites have been accounted in all the selected cells. However, the incidence of fires does not necessarily mean that a specific grid cell would have a representative total area of wildfires.

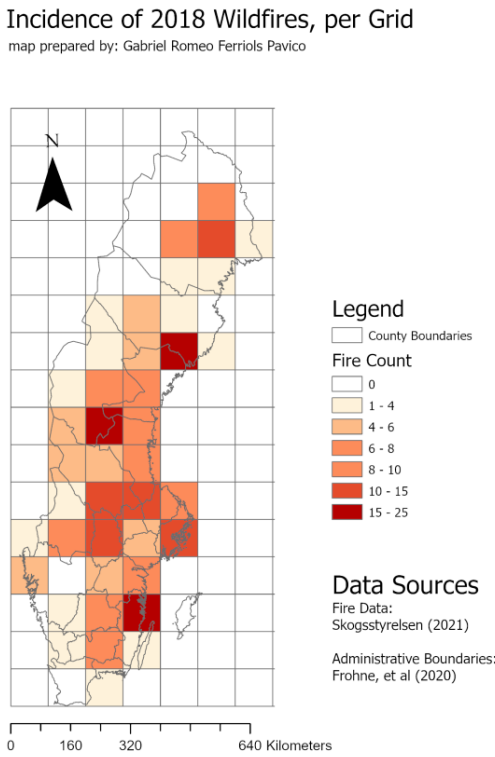

Figure 8: Incidence of 2018 Wildfires (Grid)

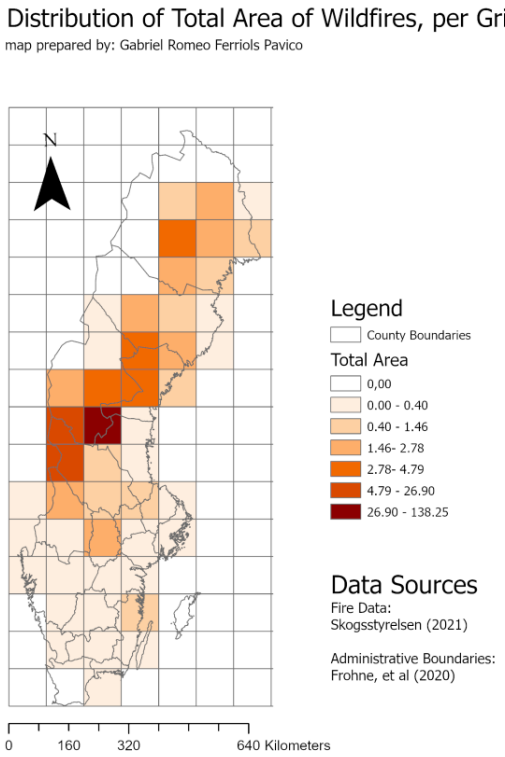

Figure 9: Total Area of Wildfires (Grid)

As seen in Figure 9, the total sizes of wildfires are highest in the midwestern part of Sweden, and the pattern spreads diagonally to the northeast. In terms of mean sizes of fires seen in each grid, as visualised in Figure 10, this ranges between 3 700 square metres (0.0037 km^2), and 6.58 square kilometres. There is a slight change in the map between the total sizes and mean sizes of wildfires. However, by having a mean area of wildfires, and after applying the logarithmic transformations, it helps in making distribution of data slightly normal; for the details of the pertinent analyses mentioned in this chapter, please see Appendix B, Test of Normality: Fire Areas, Per Grid.

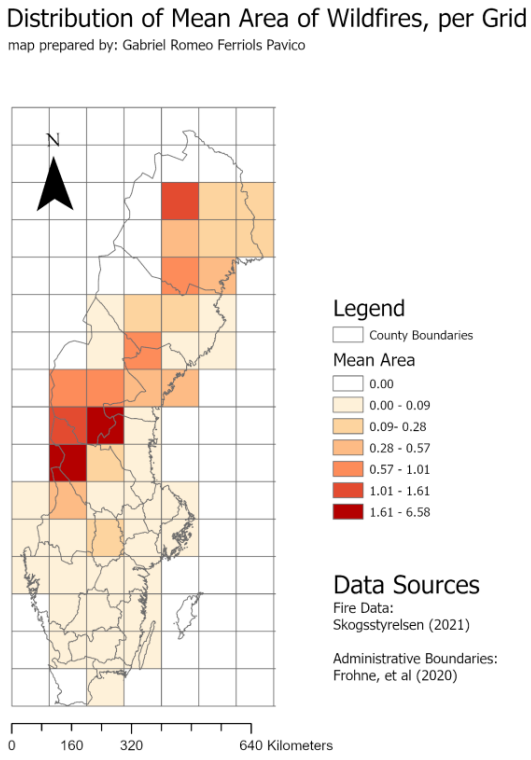

Figure 10: Mean Area of Wildfires (Grid)

Roads can be seen in 69 out of 71 grid cells, and as covered earlier, the fires that were recorded happened outside towns, hence only roads outside towns are of interest. The road density outside towns varies in cells where road features are present. The smallest amount of density is at 0.012 kilometres of road per square kilometre of land area (excluding towns), and the densest cell has 7.7 kilometres of road per square kilometre. The mean density of all cells is at 2.21 km/km^2.

When roads traverse through the land features of the three land classes, this resulted to smaller parcels of land. The mean size is taken per land classification and per cell. The average of the mean sizes of the landscape is 2.9 km^2 for forests, 0.14 km^2 for open

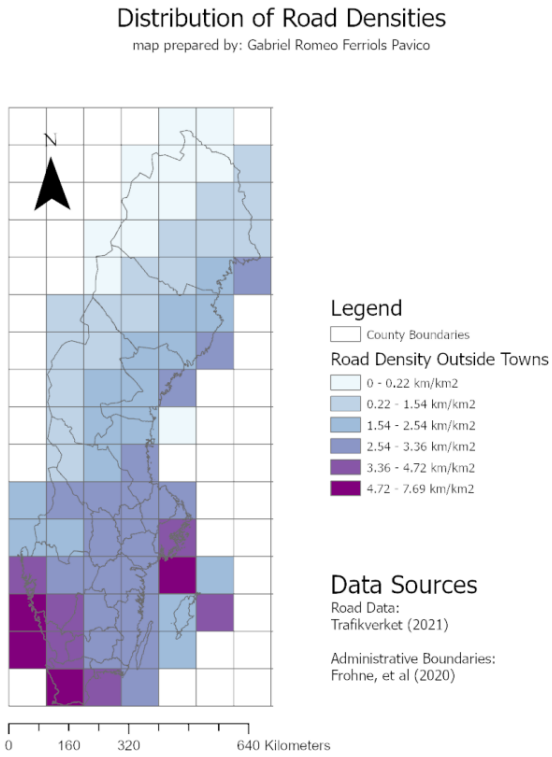

Figure 11: Distribution of Road Densities Outside Towns

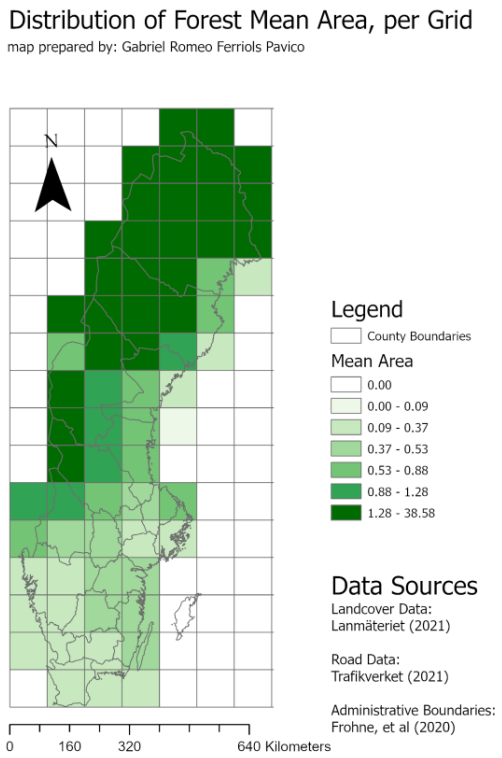

Figure 12: Distribution of Forest (Mean)

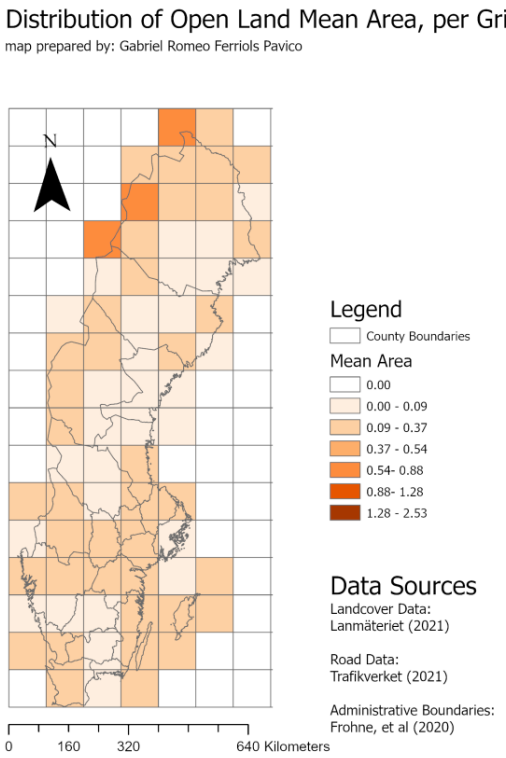

Figure 13: Distribution of Open Land (Mean)

landscapes, and 0.66 km^2 for wetlands. Although the total area of open landscapes was bigger than wetlands, when looking at the mean sizes, this suggests that roads traverse more on open landscapes resulting in smaller parcels compared to wetlands. The range of the mean sizes was uniformly set as seen in Figures 12 to 15.

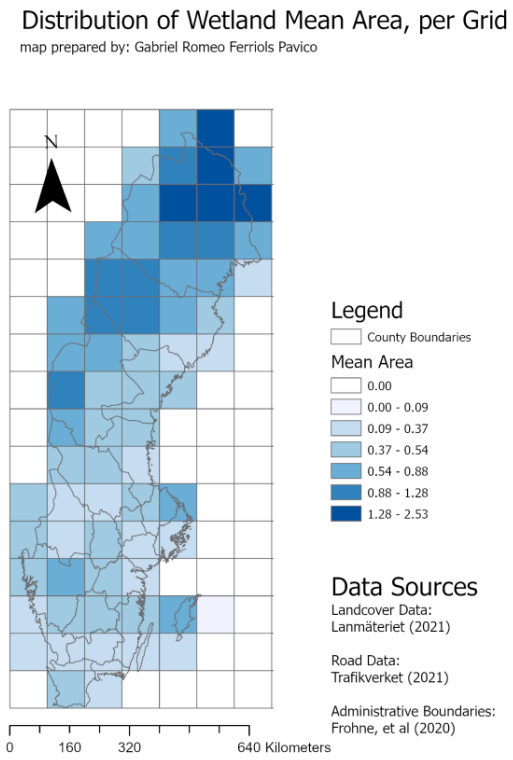

Figure 15: Distribution of Wetland (Mean)

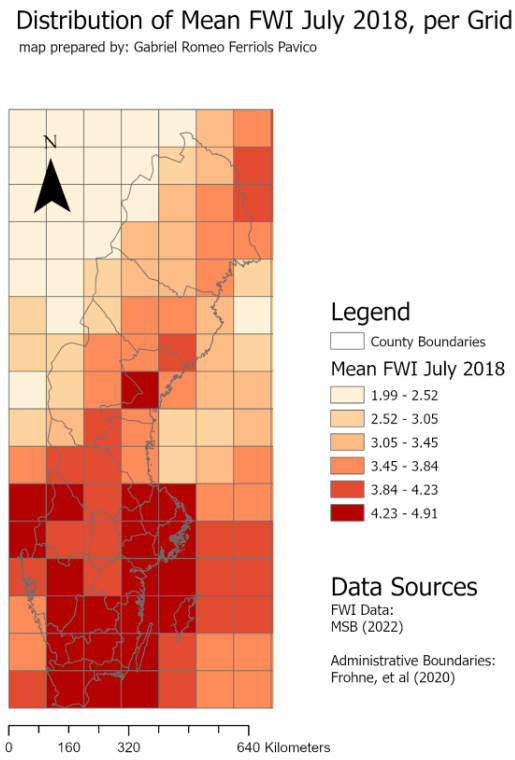

Figure 14: July FWI (Mean)

For meteorological variables, only the mean values for the month of July were observed. For values of precipitation, the country had low records of rain for the month. On the other hand, temperatures all throughout the grids were seen above the value of 15 degrees Celsius, with the mean value for all grids at 23 degrees Celsius. The Fire Weather Index is seen to be averaging at 17.50 index. Mean relative humidity is moderate, with average of 51.91% RH.

4.2 Univariate Regression Modelling

Conducting a univariate analysis helps show the linear, or one-to-one relationship (or non-relationship) between certain predictive (independent) variables and a predicted (dependent) variable. Using this testing method helps to justify the use of independent variables later in the multivariate testing. As mentioned in the methods chapter and in subsection 4.1.1, the values

recorded are not normally distributed. As a corrective measure, a logarithmic transformation (log n) was applied to the variables to create statistically sound tests from this section onward.

There are two dependent variables that will be tested: the fire area and the percent of road conformity, against some variables that have been discussed in the previous section. The univariate tests were conducted using the per site and per grid datasets to see whether trends are similar individually and if they are grouped.

However, for grid datasets, some areas would naturally record more fires which could affect the relationship between the dependent and independent variables for fires inside the grid. When comparing the results between the two dependent variables (for fire area total and area mean), the mean sizes of fires provided a better model explanation to the variances observed, through the r-squared values when paired against the tested independent variables. With this explanation and in the virtue of brevity, only the mean sizes of fires will be used as the dependent variable along with the fire area of the individual fire sites.

4.2.1 Fire area

Fire Road Density – As fires intersect with roads when the fire spreads, the longer the roads it would eventually intersect with. This is somehow tautological, and as a solution to this, fire density could be a better predictor of fire sizes. The result suggests that the higher the road density inside the fire has, the lower the fire size tends to be. Although all models provide a negative correlation, only the site dataset tested to be statistically significant, the grid dataset could be also considered to be significant in a 90% confidence interval. Given the r-square value, the model in the site dataset explains 19% of the variation in fire sizes.

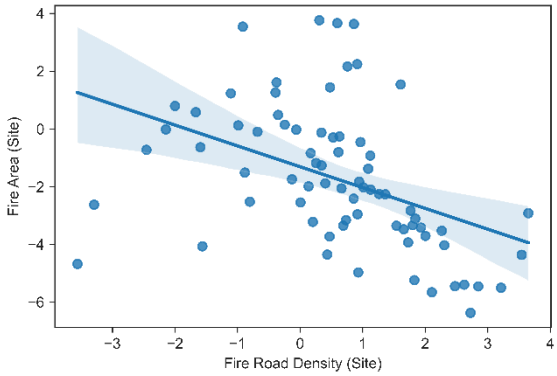

Figure 17: Fire Area v. Fire Road Density (Site)

y = -0.722 * x - 1.308

R^2 = .188 F = 16.436 (df = 1, 71) [sig, < .001]

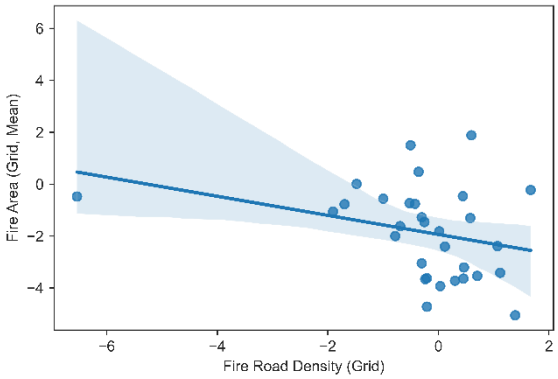

Figure 16: Fire Area v. Fire Road Density (Grid)

y = -0.368 * x + -1.939

R^2 = .090 F = 2.872 (df = 1, 29) [NS, .101]

*Definition of the notations as seen above, where: **y** – the equation of the straight-line slope (y = mx + b), **R^2** – the coefficient of determination, **F** – F-statistic, **df** – degrees of freedom, first figure being the number of independent variables, and the second as number of residuals, and **sig or NS** – Significance/Non-Significance with 95% confidence interval, unless stated. **As a logarithmic transformation was applied to normalise the distribution of data for all the variables, this resulted in ranges with negative values.

Road Conformity Percentage – As the ratio of a fire's perimeter conforming to the road increases, the smaller the fire size tends to be. Although both tests show a negative relationship with the independent variable, it was only the per site data that tested to be significant, with a significance value of less than 0.001, and a model explanation (r-square) of 26.2 percent.

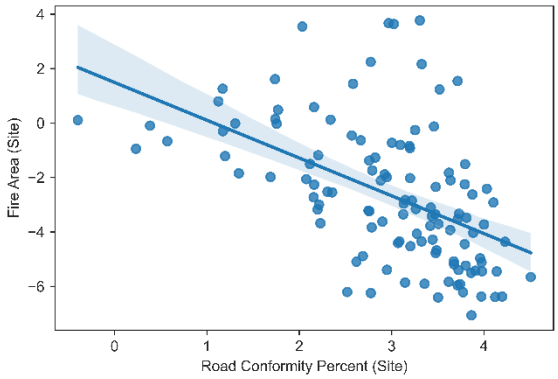

Figure 18: Fire Area v. Road Conformity Percent (Site)

y = -1.389 * x + 1.492

R^2 = .262 F = 40.505 (df = 1, 114) [sig < .001]

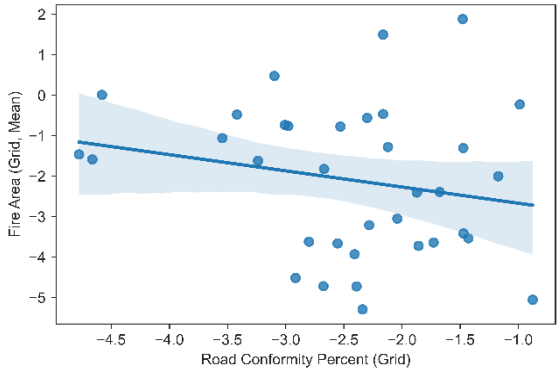

Figure 19: Fire Area v. Road Conformity Percent (Grid)

y = -0.400 * x - 3.069

R^2 = .043 F = 1.480 (df = 1, 33) [NS, .232]

Distance to Towns – The test looks at the effect of the distance to towns on the variance of fire sizes in the two datasets. Both tested to be statistically significant, with the mean distances of fires within a grid providing a better model explanation of the variances in mean fire sizes. The results suggest that the farther a fire is from a town, the larger the size of the fire will likely be.

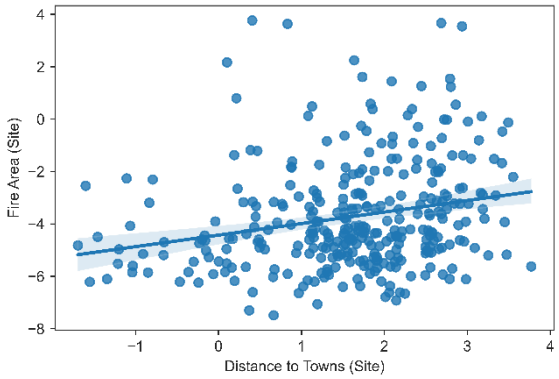

Figure 20: Fire Area v. Distance to Towns (Site)

y = 0.440 * x - 4.431

R^2 = .054 F = 18.312 (df = 1, 322) [sig < .001]

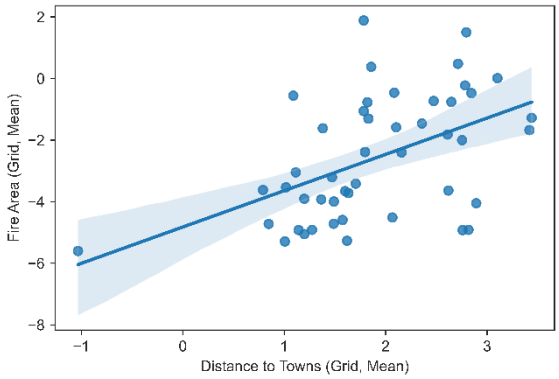

Figure 21: Fire Area v. Distance to Towns (Grid)

y = 1.179 * x - 4.825

R^2 = .243 F = 14.431 (df = 1, 45) [sig < .001]

Mean sizes of Forest in Grid – Using the mean sizes of the fires as the dependent variable against the independent variable of mean sizes of forest land, this tested to be statistically significant with a significance level of below 0.001. With the r-square, the change in mean sizes of forest land explains the 37.3% of the variation in mean fire sizes. Given the positive relationship, the larger the average sizes of forest land, the larger the expected mean size of fires will be.

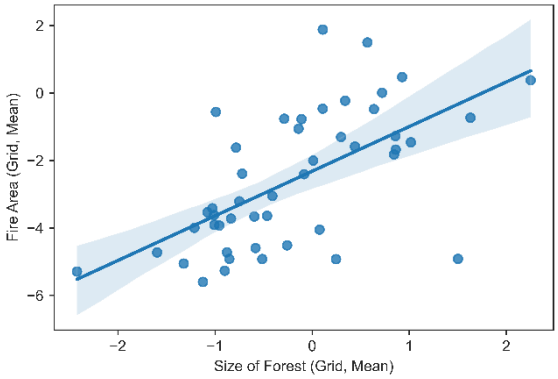

Figure 22: Fire Area v. Mean Forest Size (Grid)

y = 1.323 * x - 2.319

R^2 = .373 F = 26.773 (df = 1, 45) [sig < .001]

Mean sizes of Open Land in Grid – Using the mean sizes of open land as the independent variable did not prove to be statistically significant. Despite this, the model shows a negative relationship between mean size of land and mean size of fires in a grid cell, wherein the larger the mean sizes of open lands are, smaller average size of fires will be expected.

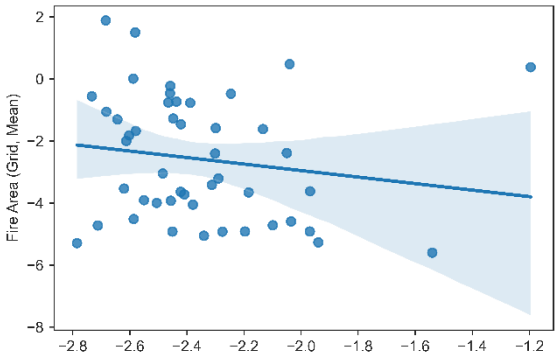

Figure 23: Fire Area v. Mean Open Land Size (Grid)

y = -1.049 * x - 5.053

R^2 = .026 F = 1.188 (df = 1, 45) [NS .282]

Mean sizes of Wetland in Grid – When tested against the independent variable, this explanatory variable is seen to be statistically significant, with the independent variable explaining the variation in mean sizes of fires at 16.6%. The test suggests that correlation between the two variables is positive; with larger mean sizes of wetland, the expected size of forest fires will be larger.

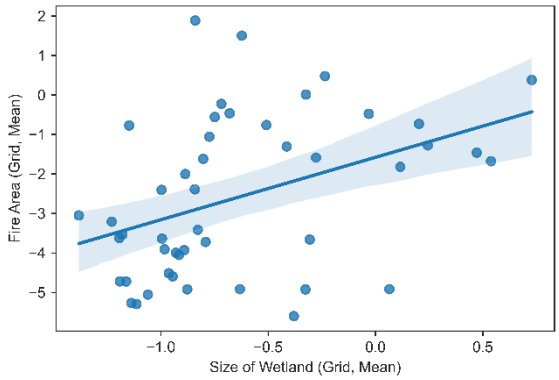

Figure 24: Fire Area v. Mean Wetland Size (Grid)

y = 1.580 * x - 1.580

R^2 = .166 F = 8.985 (df = 1, 45) [sig = .004]

Road Density Outside Towns in Grid – Since all fires, except for one, happened outside the town polygons, only roads in landscapes are selected and divided against the available landscapes. Using the road density outside towns as an independent variable, the test proves to be statistically significant when tested against the average size of fires within a grid cell. The changes in the non-town road density in a grid cell can explain the variation in average fire sizes by 24.4%.

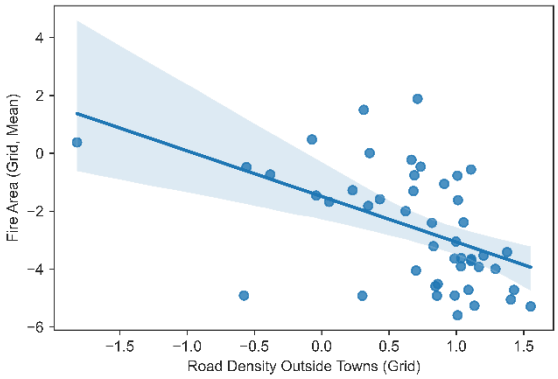

Figure 25: Fire Area v. Road Density Outside Towns (Grid)

y = -1.576 * x - 1.492

R^2 = .244 F = 14.527 (df = 1, 45) [sig < .001]

July Mean FWI – With alpha's value below the 95% confidence interval, the mean FWI values are statistically significant in predicting the variation in mean fire sizes. However, the model is showing that the directional relationship is negative, rather than positive as what previous studies suggested. This implies that the greater the FWI is, the smaller the expected mean size of fires in a grid. With its r-squared value, the model explains 16.9% of the variation of mean sizes of fires in a grid.

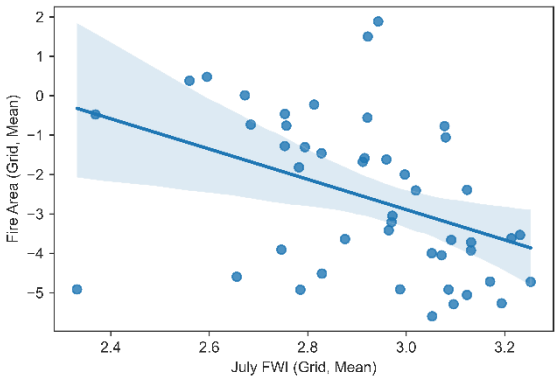

Figure 26: Fire Area v. July Mean FWI (Grid)

y = -3.84 * x + 8.64

R^2 = .169 F = 9.127 (df = 1, 45) [sig = .004]

July Mean Temperature – The mean temperature in July as an independent variable is statistically significant in predicting the variation in mean fire sizes (alpha = .031). Similar to the behaviour seen in FWI, the increase in temperature suggests a decrease in expected mean fire area. The model explains 10% of the variation of mean sizes of fires in a grid.

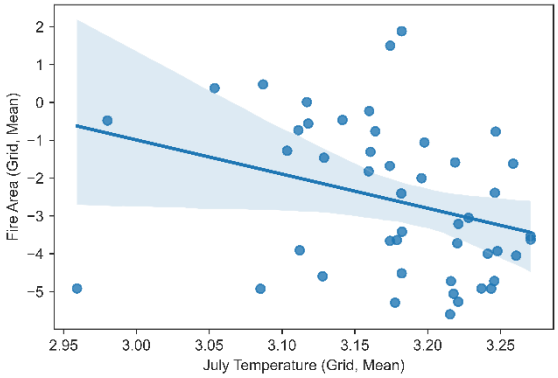

Figure 27: Fire Area v. July Mean Temperature (Grid)

y = -9.03 * x + 26.09

R^2 = .100 F = 4.973 (df = 1, 45) [sig = .031]

4.2.2 Conformity

The percentage of road conformity was seen to be statistically significant when tested against the sizes of the individual fires. For this subsection, the focus will be on the grid dataset to look at the possible explanations that could cause fire boundaries to conform to roads. There is a negative relationship between the two variables where the increase in conformity percentage of the fire would lead to an expected decrease in fire size in both datasets. This implies that when tested against the other independent variables in the earlier subsection, the relationship should be the opposite of what was seen when fire sizes were used as the dependent variable. Unlike what was shown in subsection 4.2.1, only a select number of independent variables were examined.

Distance to towns – Although statistically significant in the earlier subsection, the independent variable of distance to towns did not turn out to be statistically significant in affecting the percentage of fires conforming to roads. With its negative relationship, the further the mean distance of forest to town is in a grid, the smaller percentage of a fire is conforming. This implies that distance to towns play a role in fire suppression efforts, albeit to an insignificant degree.

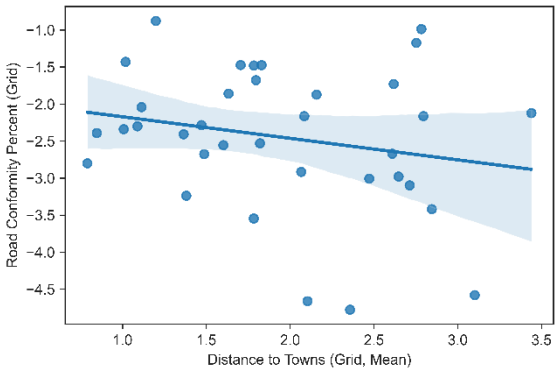

Figure 28: Road Conformity Pct. v. Distance to Towns

y = -0.291 * x -1.881

R^2 = .045 F = 1.551 (df = 1, 33) [NS, .222]

Mean sizes of Forest in Grid – The mean size of forest parcels in a grid, with a significance of below 5%, is statistically significant. However, the model only explains fourteen percent of the variance seen in the percentage of road conformity of fires with the dependent variable. The relationship between the two variables is negative; when the mean size of forest within a grid increases, the less percentage of the fire would conform to the roads (and in effect, lead to bigger fire mean sizes).

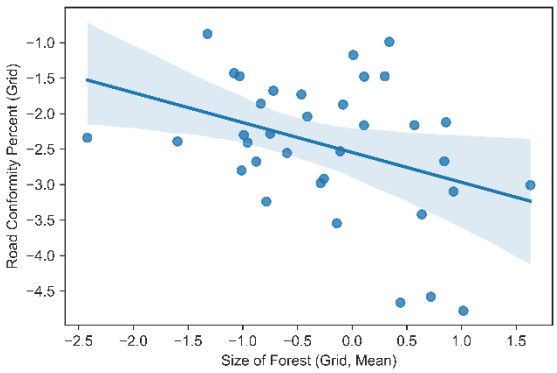

Figure 29: Road Conformity Pct. v. Forest Mean Size

y = -0.421 * x + -2.547

R^2 = .141 F = 5.438 (df = 1, 33) [sig = .026]

Mean sizes of Open land in Grid – Similar to what was observed in the earlier subsection, 4.2.1, the mean size of open land is not statistically significant in predicting the percentage of conformity of fire perimeter to roads.

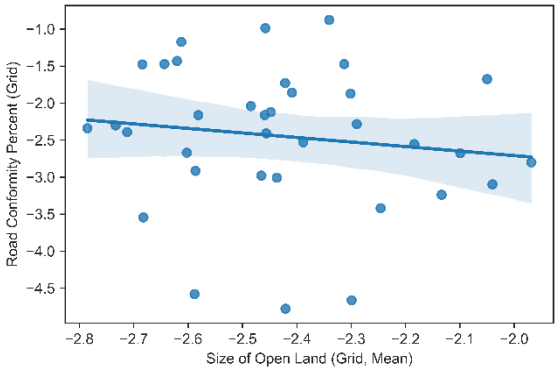

Figure 30: Road Conformity Pct. v. Open Land Mean Size

y = -0.612 * x - 3.934

R^2 = .018 F = .611 (df = 1, 33) [NS, .440]

Mean sizes of Wetland in Grid – When used as an independent variable, mean wetland sizes are statistically significant in explaining the variance seen in the percentage of conformity of fires. With a negative relationship, the model explains 24.2% of the variance in the dependent variable.

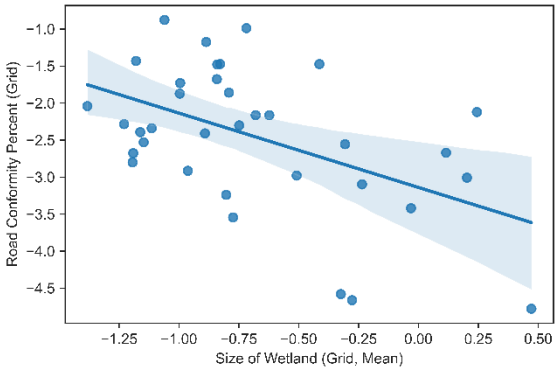

Figure 31: Road Conformity Pct. v. Wetland Mean Size

y = -1.00 * x - 3.139

R^2 = .242 F = 10.542 (df = 1, 33) [sig = .003]

Road Density Outside Towns in Grid – Yielding a significance value less than 5%, this independent variable is tested to be statistically significant with respect to the conformity percentage of wildfires. With the r-square value, the change in non-town road density of grids predicts the percentage of road conformity by 21.9 percent. The increase in the percentage of road density could be explained by the density of roads in a grid.

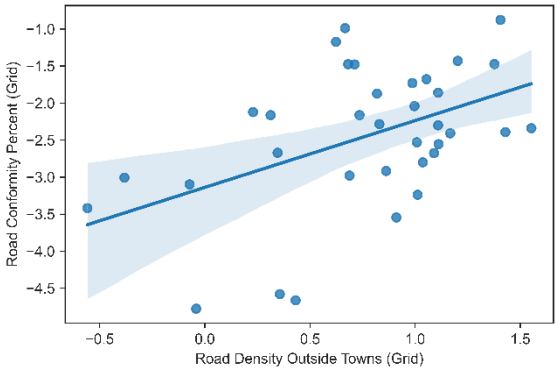

Figure 32: Road Conformity Pct. v. Road Density

y = 0.902 * x - 3.139

R^2 = .219 F = 9.261 (df = 1, 33) [sig = .005]

4.3 Multivariate Regression Modelling

4.3.1 Fire area

A multiple regression was created where the mean areas of fires was tested as a dependent variable against the following independent variables: a) mean area of forest; b) mean area of open land; c.) mean distance of fires in grid to nearest town; d.) the mean Fire Weather Index (FWI) in July, and lastly; e.) the mean temperature in July.

Table 10: Model 1 Summary, Fire Area

R	**R^2**	**F**	**df**	**Sig**
.679	.460	6.997	5, 41	< .001

Upon testing, the model of the independent variables explains 46% of the variation seen in the mean sizes of fires inside each grid cell. With the p-value being less than 0.001, far below than the threshold of 0.05, the regression model then is significant in predicting the change in the mean sizes of fires. As seen in the coefficients table (Table 11) and visualised in the partial regression plots, the variation in mean sizes of forests is significant in predicting the change in the mean sizes of fires. This relationship is positive, with an individual r-square value of 0.233. The relationship is similar to that shown in subsection 4.2.1.

For open landscapes, although testing is not significant when paired individually with mean fire sizes, the variable becomes significant when added in a regression model. The correlation, as seen in 4.2.1 is also negative, with an individual r-square value of 0.112 as seen in the partial plots. This variable was selected over wetlands since the relationship of open landscapes was different from that with forest lands.

The third independent variable, mean distance of fires in grid cell to towns, although significant when tested individually, when added in a regression model, did not prove to be significant in predicting the variations in mean fire sizes. In fact, the directional relationship changed from positive (in 4.2.1) to negative in this multivariate regression model. However, the r-square of 0.006 implies that the contribution of this is less than 1% (0.6%) which could imply that the relationship can swing either positively or negatively based on the added independent variables.

Two meteorological variables were added; the mean FWI and temperature in July to explain fire incidences inside the grid. The use of these variables could also be seen as control variables.

With both variables having significance values over 0.05, these variables are not significant enough to predict the changes in the mean sizes of fires. FWI has a negative relationship, explaining 1% of the variation in mean fire sizes. Temperature has a positive relationship, explaining 2.22% of the variation in mean fire sizes.

Table 11: Coefficients Table, Model 1

Independent Variables	Unstandardised B Coefficient	Significance	Partial Correlation (R)	Individual R^2	Collinearity, VIF
Size of Forest	1.627	.001	.483	.233	3.435
Size of Open Land	-2.043	.029	-.334	.112	1.439
Distance to Towns	-.226	.622	-.077	.006	2.757
July FWI	-1.806	.525	-.100	.010	6.890
July Temp	7.347	.341	.149	.022	5.405

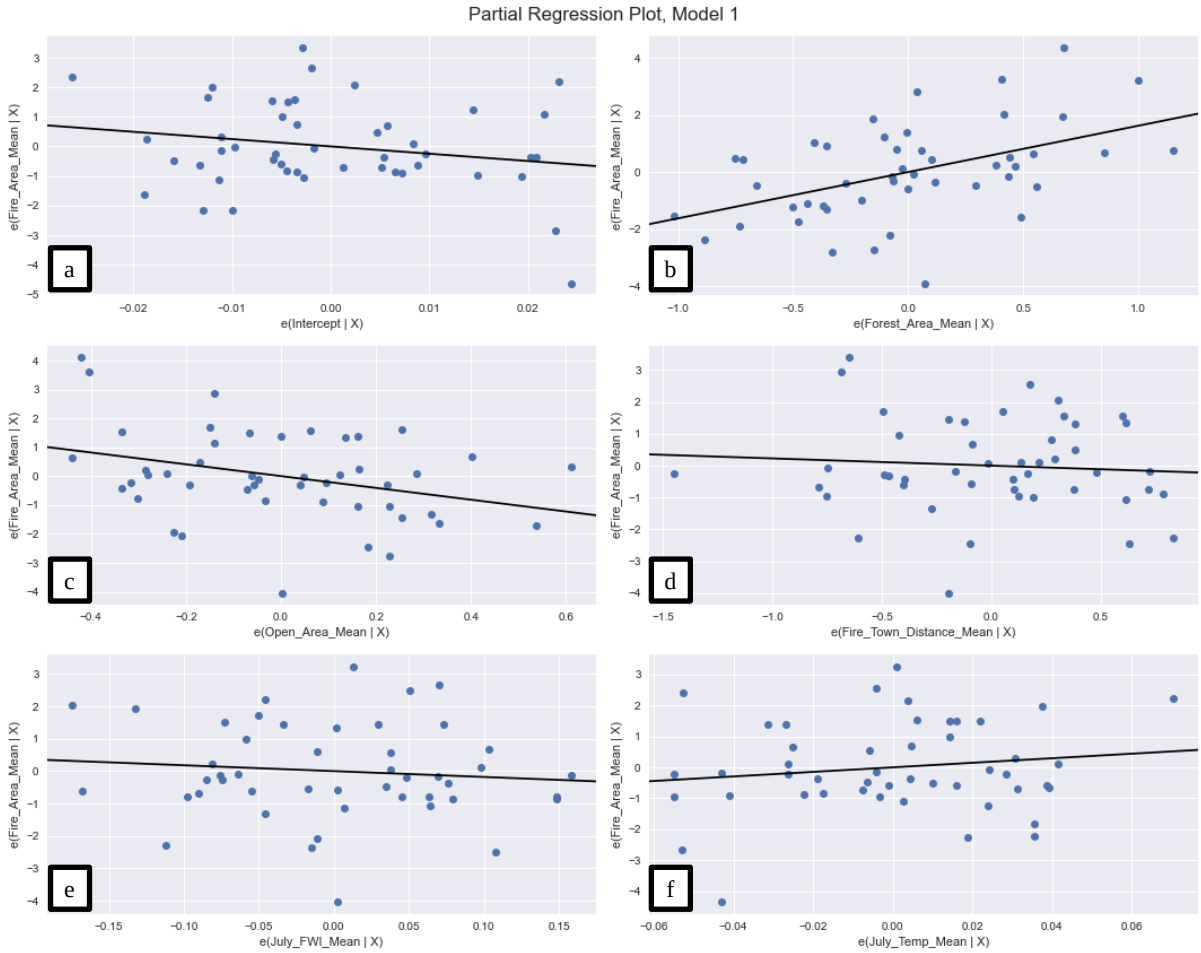

Figure 33: Partial Regression Plots, Model 1

Above are the partial regression plots for the independent variables. From left to right, top to bottom: The model intercept, mean sizes of fires (dependent variable) against mean sizes of forest, mean sizes of open land, mean distance of fires to nearest town, mean FWI value in July, and mean temperature in July. The partial plots (or added value plots) were created using statsmodels (Seabold and Perktold, 2010) but can be calculated from a regression of residuals from two models (Model 1: regression without independent variable (x_z) in question; Model 2: regression using the independent variable (x_z) as the dependent variable, against the other independent variables).

Using the calculation presented in the methods chapter, a new variable is created to provide a prediction of grids that would run the risk of larger mean fire sizes. Where a grid's log(n) value (x) for the independent variable i is multiplied by its beta coefficient (β), and further multiplied by its individual r-squared (R^2) to provide the weighting of variable i. This process is then repeated for all independent variables in the model, and eventually summed together to form a predicted value for the risk in terms of Mean Fire Area.

$$Risk = x_i \cdot \beta_i \cdot R_i^2 + x_{i+1} \cdot \beta_{i+1} \cdot R_{i+1}^2 + \ldots + x_k \cdot \beta_k \cdot R_k^2$$

Equation 2: Consolidation of x in model (reprise)

The calculation produces the following map:

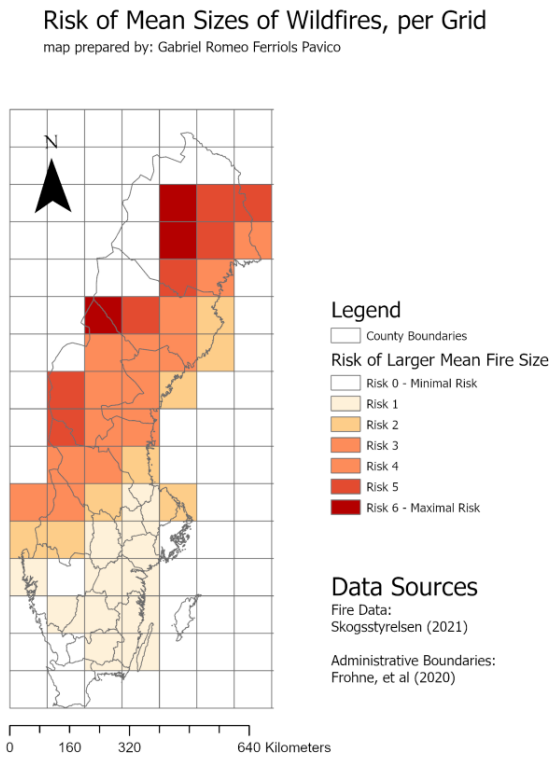

Figure 34: Risk of Mean Sizes of Wildfires

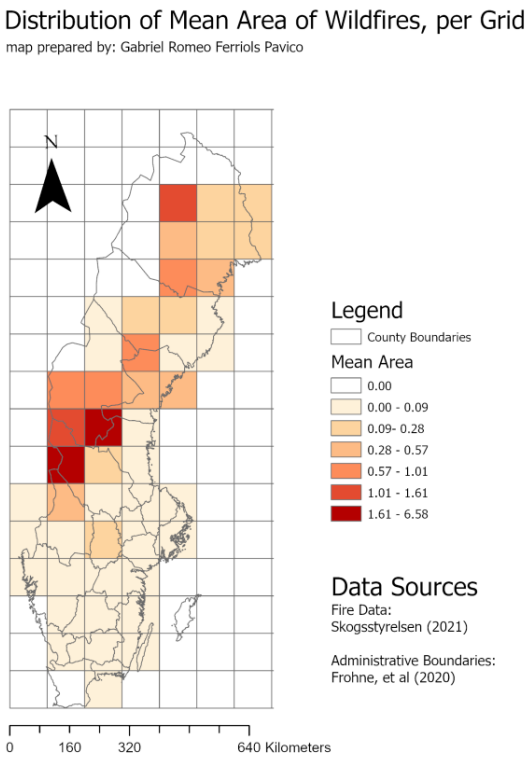

Figure 35: Mean Area of Wildfires (Grid) (reprise)

Comparing Figure 34 with Figure 35, which was presented in 4.1.2 (as Figure 10), the predicted Map somehow exaggerates the risks compared to what transpired in 2018. Despite this, the maps are in accordance when it comes to low-risk zones. Given the coefficient of determination (R^2 = .46), the predictive map could account for to almost half of the variation in wildfires that transpired in 2018.

4.3.2 Road Conformity

For this subsection, the aim is to understand what causes fires to conform to roads. As a working theory, and relating back to subsection 4.2.2, road density in landscapes could lead to increased probability of road conformity percentage in a grid cell. It has also been established in subsection 4.1 that most of the fires happened in forest land. With this, only two independent variables will be used in this model to test the variation in conformity percentage in grid cells.

Table 12: Model Summary, Road Conformity

R	R^2	F	df	Sig
.538	.290	6.528	2, 32	.004

The model as seen in the r-square value explains 29% of the variation of seen in conformity percentage. Using the result of the ANOVA, with a significance value below 0.05, the model is statistically significant.

With the significance value of road density outside of towns being below 0.05, this is statistically significant in predicting the change in conformity percentage of fires with roads. The directional correlation is positive, similar to the univariate test in 4.2.2, but with a slightly lower r-square value of 0.289. For the independent variable total forest area in grids, with the alpha being above 0.05 but below 0.10, this can still be considered as statistically significant with a confidence interval of 90% in determining the variation in conformity percentages in roads. The relationship is also positive, with a r-square value of 0.09.

Table 13: Coefficients Table, Model 2

Independent Variables	Unstandardised B Coefficient	Significance	Partial Correlation (R)	Individual R^2	Collinearity, VIF
Road Density Outside Towns	1.167	.001	.538	.289	1.267
Forest Area	.472	.084	.301	.090	1.267

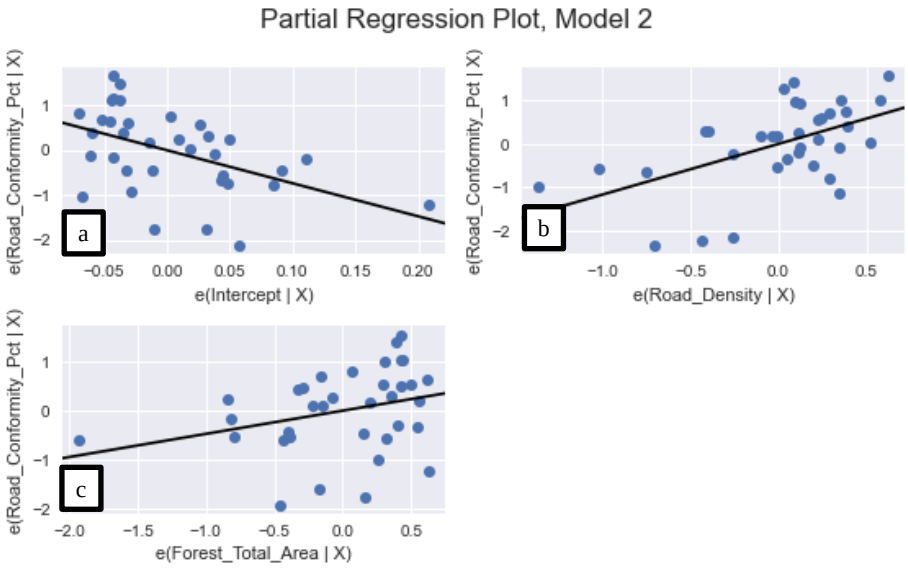

Figure 36: Partial Regression Plots, Model 2

By looking at the unstandardized b-coefficients, and with the individual r-square values in the partial regression plots, road density is a stronger driver of conformity percentage in fires. By recreating the prediction model, the following map was created:

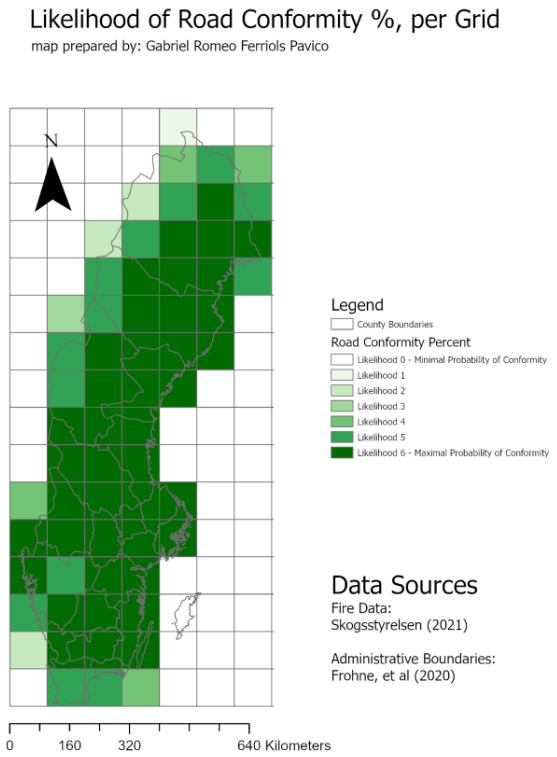

Figure 38: Likelihood of Road Conformity Percent

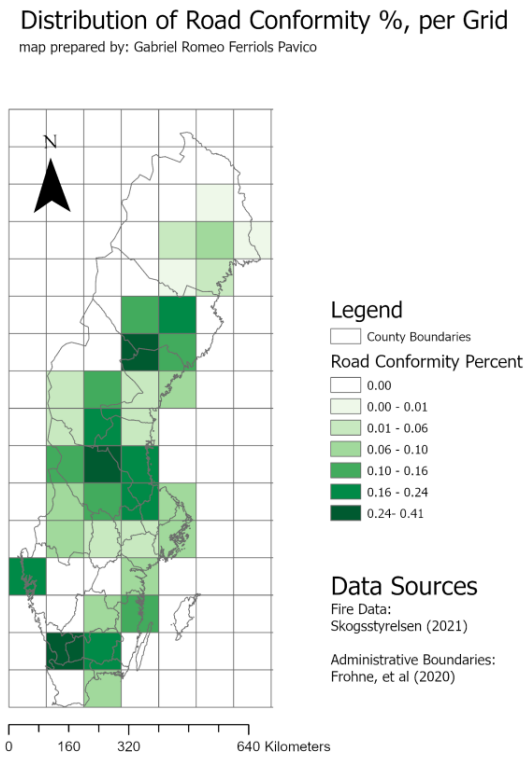

Figure 37: Distribution of Road Conformity Percent

Comparing what actually transpired in Sweden, as seen in Figure 37, to what the predicted levels of conformity is in Figure 38, the model was not able to come close to the actual levels of conformity. Even if the two variables used were statistically significant in predicting the percentage of road conformity of fires, the model is still incomplete, as seen in the map and in the R^2 value of .290. Despite these, the model could still suggest that with the amount of forests and density of roads in these grids, it could provide some idea of where fires would conform more to roads if and when they happen. And with the increased percentage of conformity, as seen in subsection 4.2.1, the smaller the fires are to be expected.

The discussion will continue in the next chapter.

5 Discussion

The study aims to observe the relationship between roads and wildfires by using Swedish wildfire data from 2018 as a case study. As this project progressed, there were several questions that needed to be addressed. The first is why was this particular year (2018) the focus of the study? As the phenomenon is temporal, this implies that there are certain variables that were unique to each period, specifically meteorological data, that allows the incidence of fires to be grouped together. As described by the government reports (Granström, 2020; SOU, 2019), 2018 was an unusually potent year when it came to wildfires when the country experienced frequent and larger fires than what were recorded in the previous years. Given the number and volume of the fire incidents, these events present an opportunity to observe the phenomenon of wildfires in an exaggerated lens. Moreover, with the realities that come along with climate change, the trends of larger wildfires could be the norm in the years to come.

The need to analyse the data per grid cell came after realising that looking at the fire sites alone will not be able to explain the phenomenon, instead the sites can only describe what already has happened. Creating a grid allows the study to look at the qualities inside the cells and find reasons why the fires happened without looking specifically at the fires. Another question that can be pointed out is that the size of the grid cells (100 x 100 km) might be too coarse. With the study being exploratory in nature, the coarseness of the grid satisfies the thesis sets out to achieve, while answering the research questions well. This opens the doors to future studies, with a tighter grid network as an example.

In terms of the reliability of data, there needs to be an assumption that the files received from the various government agencies are reliable. There are several points where errors could originate: the fire polygons, road lines, landcover polygons (including towns), and meteorological observations. In the process of creating the fire data, as manual work was conducted, there could be a tendency of errors and biases to occur, affecting the accuracy of data. As mentioned in the Methodology chapter, there was an erroneous feature in the fire dataset where a single feature ID had two polygons that are far from each other. Given the occurrence of this, digitisation errors are probable in other features within the fire dataset and even in the other datasets. In terms of biases, there is a chance that the contours of the fires were digitised given that recognisable shapes are easily seen in areas close to roads when looking at satellite images. However, having a error-free dataset is an ideal that is quite hard to

obtain, reflecting on the accuracy and being critical on the data received is important to have when doing the study. Although the results shown in the previous chapter answers the research question that was set in the study, it can only work with the assumption that the data is as close to error-free as possible.

Another aspect in the dynamics of wildfires is the suppression, in which unfortunately no data was available. As suppression efforts done by air were essential according to Granström (2020), it would be interesting to know the result of the 2018 fire season if this effort was not done at all. It will be bigger, but a question is how big would it be? On the other hand, it would also be interesting to see the land efforts done and find a way to quantify or document the efforts in a dataset. It would have added another layer in the role of roads in the spatial patterns of wildfires. In here, another assumption is made, that roads stood as access corridors for fire suppression by land.

After clearing up these initial issues, we can proceed to the research question.

5.1 Do roads influence the burned area?

Considering the fires have either intersected with roads, and or its perimeter have conformed to the roads, these incidents make up 95% of the total burned area in Sweden in 2018. By comparing the results of fires that had conformity to those that did not, there is an idea that as a fire develops through spreading, at some point it would eventually interact with a road segment. And when this happens, there are three possible scenarios that could happen. The first is that a fire would have no more potential fuel to spread to the other side of the road, and eventually start conforming its perimeter to the contours of the road, acting as a fire break. A second scenario is that the fire spreads over to the other side of the road. Despite the absence of data, there is a third scenario wherein roads act as access points in fire suppression efforts, which would in turn keep the fires from burning over to the other side of the roads and containing them on one side. In these scenarios, the more roads that are present in the path of the fires, the smaller the fire tends to be.

This notion can be explained in the univariate models of fire size against percentage of road conformity and road density inside fires. This is also in alignment in the findings seen by Pinto

et al. (2020) and Fox *et al.* (2018) where areas of high road density would eventually translate to smaller fire areas.

A possible explanation for the percentage of road conformity being a driver to fire sizes is also touched upon by Narayanaraj and Wimberly (2013) where the probable change in the volume of vegetation close to road segments to provide some clearing for vehicles and for other reasons and with such changes could affect how fires behave when interacting with roads. Another effect of the roads could be that it acts as a fuel break for eventual containment of fires (Pinto *et al.*, 2020; Forman and Alexander, 1998). This goes to show that the effect of roads, both the intersected (fire road density) and the percentage of conformity of roads, have an influence in the sizes of the fires once fires start to interact with roads.

The majority of the fires burned forest land, with an 88% intersection of all fires extent with this land cover. On the other end of the scale are open landscapes to which less than 1% of the total fire area can be attributed. As a specific fire can simultaneously burn different landcovers, the average burn percentage was still highest in forests and the least in open landscapes. Adding to this, roads would cut through the different landcovers, turning the landscapes into smaller parcels of continuous landscapes.

By breaking down into smaller parcels of land, this could be used in the model as this can replace the effect of the roads, and the effect of the landscapes. In the univariate testing, the mean sizes of forest parcels in the grid are statistically significant with a positive correlation with the average fire areas in the cell. For open lands, although not considered to be statistically significant, the effect of this is negative with the average fire areas. This behaviour seen in forest parcels was also suggested in Narayanaraj and Wimberly (2012) where fires tend to be larger when the landscape is unfragmented.

A fire's distance to towns was also seen to be statistically significant at the univariate level. The idea behind using this as a model is that the nearer a fire is to a town, the earlier detection will be, and efforts to suppress these fires by land or air would be expedient, making fire areas smaller (Narayanaraj and Wimberly, 2012). Maybe a classification of towns, such as population density, as what Pinto *et al.* (2020) and Mundo *et al.* (2013) mentioned, would be a better predictor as resources for fire mitigation and fighting would greatly differ in the sizes of towns.

The average values for the Fire Weather Index and Temperature were used in the model as these could prove to be useful variables as seen in several studies (Vitolo *et al.*, 2019; Pagnon Eriksson and Johansson, 2020). Temperature was still added as its own independent variable as Krikken *et al.* (2021) alluded that it could have an effect that could explain the fire patterns. When these were tested individually against fire areas, both variables tested to be statistically significant, but with a negative directional relationship with the dependent variable. This meant that as the index and the temperature increase, the mean fire area in a grid is expected to be smaller. This seemed to be antithetical to the different studies, but simultaneously agrees with Gomes (2022) and Fox *et al.* (2018) with the erratic effects of FWI to fire sizes. A probable reason here is that the mean of the mean was used. The mean values of FWI and temperature were used as point layers to be interpolated to a raster layer, and through the grid, the mean value was again derived. Whereas in Krikken *et al.* (2021), the other Swedish 2018 wildfire study, they utilised the maximum values of the weather stations. Being as it may, these two variables were still considered to see if there is any effect to the size of the fire area when added as part of the model.

After running the multivariate regression analysis, it was only the parcel sizes of the two landscapes (forest and open landscapes) that tested to be statistically significant in the model in predicting the variance of mean fire sizes inside the grid cells. Similar to the univariate testing, the increased mean parcel sizes of forests would predict an increase in the mean sizes of fires in a grid. Furthermore, the inverse is true with open landscapes with increased mean sizes of this land cover would translate to smaller mean sizes of fires in a grid. A probable cause for this is that the increase in the mean size of one landcover could mean a smaller mean size of the other landcover inside a grid. And given the relationships seen in the univariate regression, the quality of burnable energy available in forests and open land differ dramatically in determining fire sizes. Wetlands, which are not included in the model could be seen to have the same effect with forests when included in the model as it shares the similar relationships and statistical significance with forests. Looking at the individual r-square values for these two variables, the mean size of forests could explain the change in fire mean sizes by 23 percent, while mean sizes of open landscapes explaining by 11 percent. From a logistical perspective, the bigger the forest parcel is, the harder the detection would be, and once in the parcel, fire fighters would need to go through the different materials and obstacles present between the road and the fire. In the case of open landscapes, detection would be quicker and the absence of obstacles between the road and fire makes the suppression more expedient.

The mean distance of fires to its closest town, which was statistically significant with a positive relationship to fire sizes, proved to have no statistical significance when included in the model. In fact, the directional relationship changed when included in the model.

The Fire Weather Index was not statistically significant when added to the model. As discussed by Gomes (2022) in their master's thesis study on fires in Portugal, the researcher noticed that FWI was more prominent in fire prediction in the mid-range, than in the lower and higher ranges. In the same manner, using the independent variable of mean temperature in July was also not statistically significant. What is different however for the temperature is that the directional relationship changed from negative in the univariate testing to a positive relationship when added in the multivariate model.

The entire model explains 46% of the variation in the mean sizes of fires per grid despite only seeing a statistical significance in the mean sizes of the parcels of forests and open landscapes. This strengthens the idea that a) **landcovers play a role in the sizes of the fires**, and moreover, b) **the presence of roads cutting through the different land covers creating smaller parcels of land, inadvertently influences the outcome of fire sizes in a grid**.

For the second model in the variation in percentage of road conformity, the average percentage of conformity of affected fires is seen at 26.79%, which is in line with the average relative conformity in Yocom *et al.* (2019) at 25.7%. Randomly or by chance, the conformity percentage is seen at 14 percent. In the univariate testing, the road density, plus the mean sizes of forests and wetlands had statistical significance in predicting the variation seen in the percentage of conformity with roads in a grid. However, both road density and mean sizes of parcels are derived from the presence of the roads. By putting both variables in a model, it would be hard to see which really drives the change in conformity. To be able to have roads and landscapes as separate variables, the solution was to use the road density (outside of towns) as one variable, and the total amount of forest area in a grid as another variable.

As what was discussed, most of the land burned was forest land, and it was interesting to see a simple model that involved the two strong drivers for fire area (being landcover and roads) but looking at the relative conformity of the fires to the roads. After running the multivariate regression model, with the r-square value, the model explains 29% of the variation seen the percentage of conformity in the grid network. On both accounts, the density of road networks and the total area of forest land were tested to be statistically significant in influencing the

relative conformity of fires, albeit in total forest area where the confidence interval was lowered to 90% to be considered to be statistically significant. Both variables showed a positive correlation in influencing the dependent variable which is the percent conformity in a grid.

What was interesting is that the total area of forests drives the spread of fire given the quality of potential fuel in the area, and at the same time the denseness of the road network somehow curbs the fires. This time, **the presence of the roads helps shape the final shape of fires**. By looking at the predictive map that was created from the multivariate model, and seeing the relatively low r-square value of 0.29, This model acts as the inverse of that of Krikken *et al.* (2021), where they mentioned the importance of other factors such as topography in explaining the narrative of fire behaviour. For the case of the model, as meteorological observations were not considered, this provided an incomplete picture in the narrative of fire behaviour. Other variables could be examined in future studies on fire perimeter conformity, such as the slope, aspect, or wind direction as potential points to examine.

5.2 Summary

In this thesis study, we see that the presence of roads could act as fire breaks, hindering the spread of fire as seen in the road density, through parcels of landscapes and in the road conformity of the 2018 wildfires in Sweden. Adding to this, the presence of roads could act as access points in fire suppression efforts.

From the different tests performed, we see that roads influence the burned area in different ways. Roads could act as fire breaks, as seen in the eventual road conformity of the fire's perimeter. With the increased percentage of road conformity, smaller sizes are to be expected. In the case of Sweden, the presence of forests drives the spread of fires, but as roads traverse through forests, this cuts the landscape into smaller parcels. With smaller parcels of forests, smaller fires are also to be expected.

The first model can help planners pinpoint areas that could be at risk of having bigger fires from their landscape parcels, while the second helps pinpoint areas that have the potential of curbing fires via the road density and potential burnable materials in an area.

Through the course of this study, several variables were used and created and given an exploratory approach. These were then tested out, some blindly, but some with a theoretical

reasoning behind their application. The researcher feels that the study satisfies the questions that needed to be answered and helps provide some new insights in the growing literature on wildfires and their behaviour.

6 Conclusion

By focusing on the 2018 Swedish Wildfire events, this study explored the influence of roads on the spatial patterns of fire sites. The thesis project explored a broad research question by using road data to transform and manipulate the three landcovers of forests, open landscapes, and wetlands, along with other variables such as distance to towns, FWI and temperature.

Two datasets were created, the individual fire site data describes what transpired and a grid data to help predict and explain why such events happened. Using the three statistical testing methods, there were several realisations that surfaced. As a fire spreads more into the landscapes, the probability of interacting with roads increases. Fire sites representing 95% of the total burnt area were seen to have interacted with roads to varying degrees.

There are three scenarios when fires interact with roads: a) that fires would lose access to burnable materials, acting as a fire barrier; b) fires spread to the other side of the road as seen in roads inside the fire area, and; c) as roads act as a corridors for manual fire suppression by land, although no data to support this in the study.

Landscapes coupled with roads, are drivers in determining fire sizes. By turning landscapes into smaller parcels using road data, it was shown that the smaller the mean sizes of forests are in a grid, the smaller the mean sizes of fires are to be expected. The type of landscape is important to look at, as open landscapes, given the relative sparsity of vegetation, provides a negative correlation between mean size of landscape and mean size of fires. Variables such as mean distance of fires to towns, mean FWI and temperature in July were, seen to be statistically significant in univariate testing, but do not test to be statistically significant in the multivariate model.

When observing the fire sites, there was a realisation that some fires tend to conform their perimeters with road features. When tabulating the data, there was an average of 26.79% in road conformity among selected fires with conformity. The results in univariate testing proved that the increased percentage of conformity of a fire would lead to smaller fire sizes. In the multivariate model, both road density (outside towns) and total forest area in a grid were found to be statistically significant, at the 95 and 90% confidence intervals respectively. The density of road features in a grid heightens the tendency for fires to increase their relative conformity to roads. This leads to smaller predicted mean sizes of fires.

7 References

Banerjee, S., Das, D. and John, R. (2021) 'Grassland vegetation and roads have dominant influence on decadal-scale spatial-temporal patterns of fires in a species-rich protected Terai habitat in northeastern India', *Agricultural and Forest Meteorology*, 304-305.

Cook, L. (2022) 'EU report: Drought-hit Europe could face 3 more dry months', *The Washington Post*. Available at: https://www.washingtonpost.com/world/eu-report-drought-hit-europe-could-face-3-more-dry-months/2022/08/24/f7552fcc-239f-11ed-a72f-1e7149072fbc_story.html.

Dewberry, S. O. (2008) *Land development handbook. planning, engineering, and surveying.* 3rd ed. edn.: McGraw-Hill.

Ekonomifakta (2022) *BNP, år, miljarder kronor*. Stockholm: Ekonomifakta. Available at: https://www.ekonomifakta.se/Fakta/Ekonomi/Tillvaxt/BNP---Sverige/?graph=/14515/1/all/ (Accessed: Sep 13, 2022).

Eriksson, S., Lasell, A., Sandgren, M., Gunnarsson, S., Nymark, E. and Larsson, S. (2018) *Slutrapport avseende: Kartläggning av skador på transportinfrastruktur med anledning av skogsbränderna sommaren 2018*, Gävle: Trafikverket (TRV 2018/90505). Available at: https://www.diva-portal.org/smash/get/diva2:1425687/FULLTEXT01.pdf.

Forman, R. T. T. and Alexander, L. E. (1998) 'Roads and Their Major Ecological Effects', *Annual Review of Ecology and Systematics*, 29, pp. 207-231.

Fox, D. M., Carrega, P., Ren, Y., Caillouet, P., Bouillon, C. and Robert, S. (2018) 'How wildfire risk is related to urban planning and Fire Weather Index in SE France (1990–2013)', *Science of the Total Environment*, 621, pp. 120-129.

Frohne, E., Runfola, D., Anderson, A., Baier, H., Crittenden, M., Dowker, E. and Fuhrig, S. (2020) 'geoBoundaries: A global database of political administrative boundaries.' [Map Data, SWE-ADM1-68755315], e0231866, P.O. Available at: https://doi.org/10.1371/journal.pone.0231866. (Accessed: Feb 01, 2022).

Gomes, L. F. (2022) *The influence of climate, population density, tree species and land cover on fire pattern in mainland Portugal.* Master in Geographical Information Science, Lund University, Lund.

Granström, A. (2020) *Brandsommaren 2018 – Vad hände, och varför?* , Umeå: Institutionen för skogens ekologi och skötsel, SLU. Available at: https://rib.msb.se/filer/pdf/29059.pdf.

Houghton, J. T. (2015) *Global warming : the complete briefing.* 5. ed. edn. Cambridge, UK: Cambridge University Press.

Huisman, O. and de By, R. A. (eds.) (2009) *Principles of Geographic Information Systems: An introductory textbook.* 4 edn. Enschede: International Institute for Aerospace Survey and Earth Sciences (ITC).

Hunter, J. D. (2007) 'Matplotlib: A 2D graphics environment', *Computing in Science & Engineering*, 9(3), pp. 90-95.

IPCC (2007) *Climate Change 2007: Synthesis Report. Contribution of Working Groups I, II and III to the Fourth Assessment Report of the Intergovernmental Panel on Climate Change* Geneva, Switzerland: IPCC.

Krikken, F., Lehner, F., Haustein, K., Drobyshev, I. and Oldenborgh, G. J. v. (2021) 'Attribution of the role of climate change in the forest fires in Sweden 2018', *Natural Hazards and Earth System Sciences*, 21, pp. 2169-2179.

Krisinformation.se (2018) *Skogsbränderna 2018*: Myndigheten för samhällsskydd och beredskap. Available at: https://www.krisinformation.se/detta-kan-handa/handelser-och-storningar/2018/brandrisk2018 (Accessed: Jan 25 2022).

Lantmäteriet (2021) 'GSD-General Map Vector' [Map Data], Lantmäteriet (Accessed: Feb 16, 2022).

Laschi, A., Foderi, C., Fabiano, F., Neri, F., Cambi, M., Mariotti, B. and Marchi, E. (2019) 'Forest road planning, construction and maintenance to improve forest fire fighting: A review', *Croatian Journal of Forest Engineering*, 40(1), pp. 207-219.

Lawson, B. D. and Armitag, O. B., Canadian Forest Service Northern Forestry Center (2008) *Weather Guide for the Canadian Forest Fire Danger Rating System.* Edmonton, Canada: Natural Resources Canada.

Leonard, B., Plantinga, A. J. and Wibbenmeyer, M. (2021) 'Stranded land constrains public land management and contributes to larger fires', *Environmental Research Letters*, 16(11), pp. 114014.

Molina, J. R., Lora, A., Prades, C. and Rodríguez y Silva, F. (2019) 'Roadside vegetation planning and conservation: New approach to prevent and mitigate wildfires based on fire ignition potential', *Forest Ecology and Management*, 444, pp. 163-173.

Mundo, I. A., Wiegand, T., Kanagaraj, R. and Kitzberger, T. (2013) 'Environmental drivers and spatial dependency in wildfire ignition patterns of northwestern Patagonia', *Journal of Environmental Management*, 123, pp. 77-87.

Myndigheten för samhällsskydd och beredskap (2022) 'Brandriskvärden juni-juli 2018' (Accessed: Mar 08, 2022).

Narayanaraj, G. and Wimberly, M. C. (2012) 'Influences of forest roads on the spatial patterns of human- and lightning-caused wildfire ignitions', *Applied Geography*, 32(2), pp. 878-888.

Narayanaraj, G. and Wimberly, M. C. (2013) 'Influences of forest roads and their edge effects on the spatial pattern of burn severity', *International Journal of Applied Earth Observation & Geoinformation*, 23, pp. 62-70.

Newsome, D., Moore, S. A. and Dowling, R. K. (2013) *Natural area tourism: ecology, impacts and management. Aspects of tourism: 58.* 2nd edn. Bristol, UK; NY, USA; Ontario, Canada: Channel View Publications.

Pagnon Eriksson, C. and Johansson, N. (2020) *Review of wildfire indices: Indices applicable for a Swedish context* [Report], Lund: Division of Fire Safety Engineering, Lund University. Available at: https://ludwig.lub.lu.se/login?url=https://search.ebscohost.com/login.aspx?direct=true&AuthType=ip,uid&db=edsswe&AN=edsswe.oai.lup.lub.lu.se.404387de.8dd1.4b72.9c45.fe3e4f431048&site=eds-live&scope=site.

Pew, K. L. and Larsen, C. P. S. (2001) 'GIS analysis of spatial and temporal patterns of human-caused wildfires in the temperate rain forest of Vancouver Island, Canada', *Forest Ecology and Management*, 140(1), pp. 1-18.

Pinto, G. A. S. J., Rousseu, F., Niklasson, M. and Drobyshev, I. (2020) 'Effects of human-related and biotic landscape features on the occurrence and size of modern forest fires in Sweden', *Agricultural and Forest Meteorology*, 291, pp. 108084.

Seabold, S. and Perktold, J. 'statsmodels: Econometric and statistical modeling with python', *9th Python in Science Conference*, 2010.

Skogsstyrelsen (2020) 'Skogsbränder' [Map Data], Skogsstyrelsen (Accessed: Feb 01, 2022).

SOU (2019) *Skogsbränderna sommaren 2018: Betänkande av 2018 års skogsbrandsutredning*, Stockholm: Statens Offentliga Utredningar (SOU 2019:7). Available at: https://www.regeringen.se/4906d2/contentassets/8a43cbc3286c4eb39be8b347ce78da16/skogsbranderna-sommaren-2018-sou-2019-7.pdf (Accessed: Jan 24 2022).

Takacs, S., Schulte to Bühne, H. and Pettorelli, N. (2021) 'What shapes fire size and spread in African savannahs?', *Remote Sensing in Ecology and Conservation*, 7(4), pp. 610-620.

Trafikverket (2022) 'Trafiknätsdata för blåljusverksamheten' [Map Data, Region Nord, Mitt, Väst, Öst, Stockholm, Syd], Trafikverket. Available at: https://lastkajen.trafikverket.se/ (Accessed: Feb 01, 2022).

Vikström, K. (2018) 'Så mycket kan skogsbränderna kosta', *SVT Nyheter*, Available: SVT. Available at: https://www.svt.se/nyheter/lokalt/norrbotten/sa-mycket-kan-skogsbranderna-kosta (Accessed Sep 19, 2022).

Vitolo, C., Di Napoli, C., Di Giuseppe, F., Cloke, H. L. and Pappenberger, F. (2019) 'Mapping combined wildfire and heat stress hazards to improve evidence-based decision making', *Environment International*, 127, pp. 21-34.

Wachs, M. and Schofer, J. L. (1969) 'Abstract Values and Concrete Highways', *Traffic Quarterly*, 23(1), pp. 133-156.

Waskom, M. L. (2021) 'seaborn: statistical data visualization', *Journal of Open Source Software*, 6(60), pp. 3021.

World Wildlife Fund for Nature and Boston Consulting Group (2020) *Fires, Forests And The Future: A Crisis Raging Out Of Control?* [Report], Switzerland: WWF International.

Yocom, L. L., Jenness, J., Fulé, P. Z. and Thode, A. E. (2019) 'Previous fires and roads limit wildfire growth in Arizona and New Mexico, U.S.A', *Forest Ecology and Management*, 449, pp. 1-7.

Appendices

Appendix A – Python Scripts

Script 1: Weather Kriging

```
import arcpy

from arcpy import env

arcpy.env.workspace = 'D:/OneDrive - Lund University/Map Files/13 -
Thesis/Road_Density2.gdb'

# featureClassList = arcpy.ListFeatureClasses()

with arcpy.EnvManager(extent="245167,77930309 6132288,34679233 1079706,17683153
7688269,30994789"):
    for i in range(24,31):
        print(f'Brandrisk_week_{i}')
        arcpy.ddd.Kriging(fr"Brandrisk_week_{i}", "Nederbord", fr"D:/OneDrive - Lund
University/Map Files/13 - Thesis/Road_Density2.gdb/Brandrisk_week_{i}_precip",
"Spherical 2593,820000 # # #", 1000, "VARIABLE 12", None)
        print('Done precip')
        arcpy.ddd.Kriging(fr"Brandrisk_week_{i}", "Temp", fr"D:/OneDrive - Lund
University/Map Files/13 - Thesis/Road_Density2.gdb/Brandrisk_week_{i}_temp",
"Spherical 2593,820000 # # #", 1000, "VARIABLE 12", None)
        print('Done temp')
        arcpy.ddd.Kriging(fr"Brandrisk_week_{i}", "FWI", fr"D:/OneDrive - Lund
University/Map Files/13 - Thesis/Road_Density2.gdb/Brandrisk_week_{i}_fwi", "Spherical
2593,820000 # # #", 1000, "VARIABLE 12", None)
        print('Done fwi')
        arcpy.ddd.Kriging(fr"Brandrisk_week_{i}", "FWI_Index", fr"D:/OneDrive - Lund
University/Map Files/13 - Thesis/Road_Density2.gdb/Brandrisk_week_{i}_fwi_index",
"Spherical 2593,820000 # # #", 1000, "VARIABLE 12", None)
        print('Done fwi_index')
        arcpy.ddd.Kriging(fr"Brandrisk_week_{i}", "Vindhastighet", fr"D:/OneDrive - Lund
University/Map Files/13 - Thesis/Road_Density2.gdb/Brandrisk_week_{i}_wind",
"Spherical 2593,820000 # # #", 1000, "VARIABLE 12", None)
        print('Done wind')
        arcpy.ddd.Kriging(fr"Brandrisk_week_{i}", "RH", fr"D:/OneDrive - Lund
University/Map Files/13 - Thesis/Road_Density2.gdb/Brandrisk_week_{i}_humid",
"Spherical 2593,820000 # # #", 1000, "VARIABLE 12", None)
        print('Done humid')
```

Script 2: Mean and Median Values for Grid Polygons:

```
import arcpy
import numpy as np
import statistics

arcpy.env.overwriteOutput = True
arcpy.env.workspace = 'D:/OneDrive - Lund University/Map Files/13 -
Thesis/Road_Density2.gdb'

# featureclasses = arcpy.ListFeatureClasses('grid_*')
featureclasses = ['grid_forest_parcels', 'grid_wetland_parcels', 'grid_open_parcels',
'grid_fire_extents2018', 'grid_connected_wetland', 'grid_connected_openland',
'grid_connected_forest']

grid = 'fishnet_sweden'

#get fields
# fields = arcpy.ListFields(grid)
# fld = []
# for field in fields:
#     fld.append(field.name)
# for quicker processing, above is skipped
fld = ['OID']


#get ID of grids
# oid = []
# with arcpy.da.SearchCursor(grid, fld[0]) as cursor:
#     for row in cursor:
#         oid.append(row[0])
# for quicker processing, above is skipped
for fc in featureclasses:
    print(fc)
    tbl = []
    for x in range(1,145):
        tbl.append(x)

    mean = []
    median = []
    for i in range(144):
        #iterate through grids
        print(tbl[i])
        select_grid = arcpy.SelectLayerByAttribute_management(grid, 'NEW_SELECTION',
f'{fld[0]} = {tbl[i]}')

        #select features in grid
        select_features = arcpy.management.SelectLayerByLocation(fc, 'WITHIN', select_grid)
        values = []
```

```
        #extract values of selected features
        for row in arcpy.da.SearchCursor(select_features, ['fid', 'area']):
            print(f'ID: {row[0]} Area: {row[1]}')
            values.append(row[1])

        #if empty values
        if len(values) == 0:
            mean.append(0)
            median.append(0)
        else:
            mean.append(statistics.mean(values))
            median.append(statistics.median(values))

    table = np.column_stack([tbl, mean, median])
    np.savetxt(f'D:/OneDrive - Lund University/Map Files/13 - Thesis/griddata/{fc}.csv',
table, delimiter=',', fmt='%.6f')
```

Script 3: Zonal Statistics for Rasters and Excel Conversion

```
import arcpy
# from arcpy.sa import *

arcpy.env.overwriteOutput = True
arcpy.env.workspace = 'D:/OneDrive - Lund University/Map Files/13 -
Thesis/Road_Density2.gdb'

# rasters = arcpy.ListRasters('Site_Brandrisk*')

# for raster in range(36,40):
#     i = rasters[raster]
#     arcpy.sa.ZonalStatisticsAsTable('fire_extents2018', 'ObjectId_1', f'{i}', f'D:/OneDrive -
Lund University/Map Files/13 - Thesis/Road_Density2.gdb/{i}_mean', "DATA", "MEAN",
"CURRENT_SLICE", 90, "AUTO_DETECT")
#     print(i)

tables = arcpy.ListTables('Site_Brandrisk*')
for i in tables:
    arcpy.conversion.TableToExcel(i, f'D:/OneDrive - Lund University/Map Files/13 -
Thesis/griddata/{i}.xls', "NAME", "CODE")
    print(i)
```

Appendix B – Statistical Tables

Test of Normality: Fire Areas, Per Site

Before logarithmic correction:

Tests of Normality

	Kolmogorov-Smirnov[a]			Shapiro-Wilk		
	Statistic	df	Sig.	Statistic	df	Sig.
Fire Area km2	.436	325	<,001	.141	325	<,001

a. Lilliefors Significance Correction

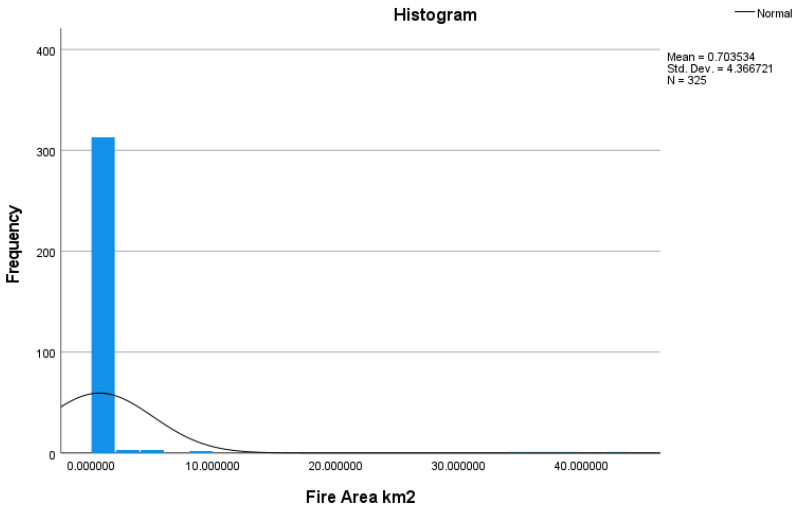

After logarithmic correction:

Tests of Normality

	Kolmogorov-Smirnov[a]			Shapiro-Wilk		
	Statistic	df	Sig.	Statistic	df	Sig.
Log Fire Area km2	.116	325	<,001	.924	325	<,001

a. Lilliefors Significance Correction

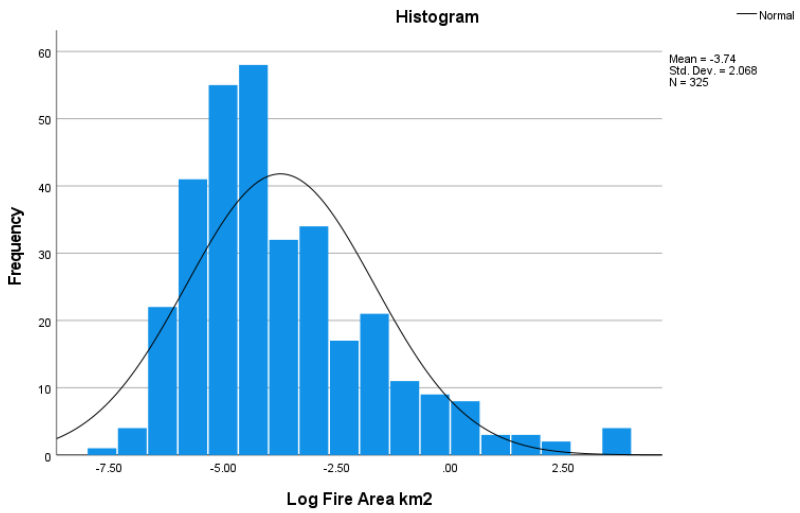

*Although the corrected variable failed the test of normality, the histogram shows how the distribution improved after the logarithmic transformation.

Test of Normality: Fire Areas, Per Grid

Before Logarithmic Correction, Fire Area Total:

Tests of Normality

	Kolmogorov-Smirnov[a]			Shapiro-Wilk		
	Statistic	df	Sig.	Statistic	df	Sig.
Fire Area km2	.438	47	<,001	.229	47	<,001

a. Lilliefors Significance Correction

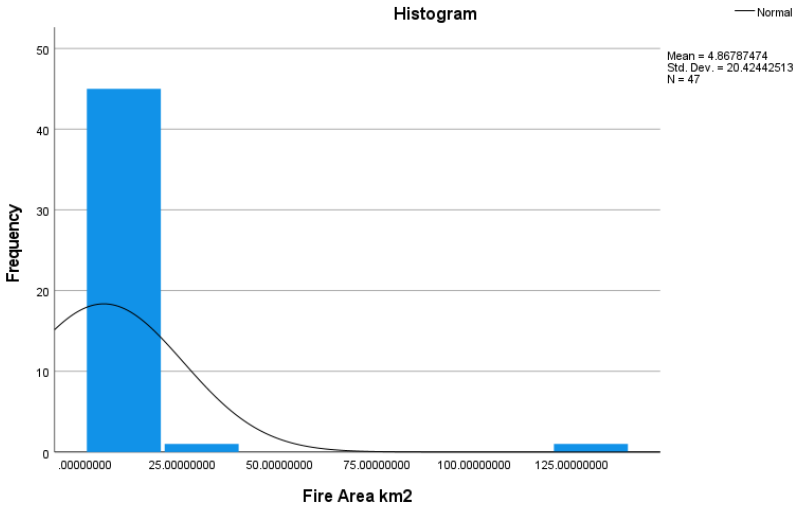

Before Logarithmic Correction, Fire Area Mean:

Tests of Normality

	Kolmogorov-Smirnov[a]			Shapiro-Wilk		
	Statistic	df	Sig.	Statistic	df	Sig.
Fire Area Mean km2	.346	47	<,001	.421	47	<,001

a. Lilliefors Significance Correction

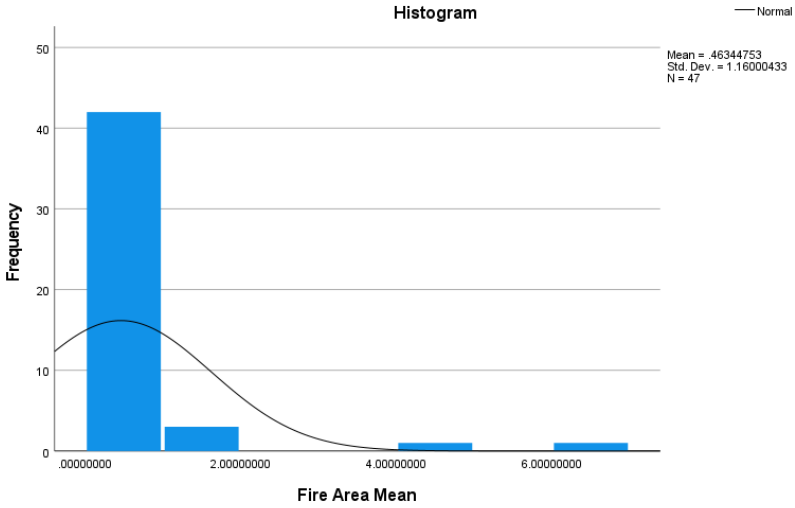

After logarithmic correction, Fire Area Total:

Tests of Normality

	Kolmogorov-Smirnov[a]			Shapiro-Wilk		
	Statistic	df	Sig.	Statistic	df	Sig.
Log Fire Area km2	.106	47	.200*	.970	47	.271

*. This is a lower bound of the true significance.

a. Lilliefors Significance Correction

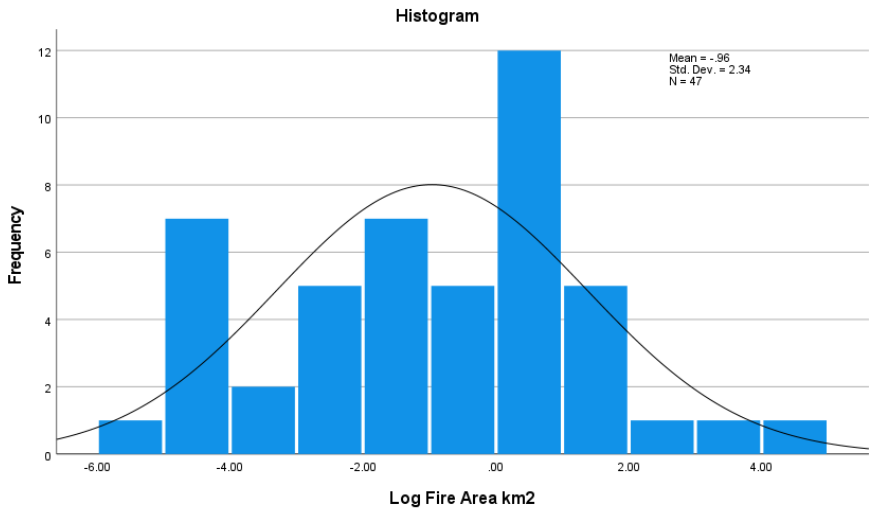

After Logarithmic Correction, Fire Area Mean:

Tests of Normality

	Kolmogorov-Smirnov[a]			Shapiro-Wilk		
	Statistic	df	Sig.	Statistic	df	Sig.
Log Fire Area Mean km2	.129	47	.047	.946	47	.030

a. Lilliefors Significance Correction

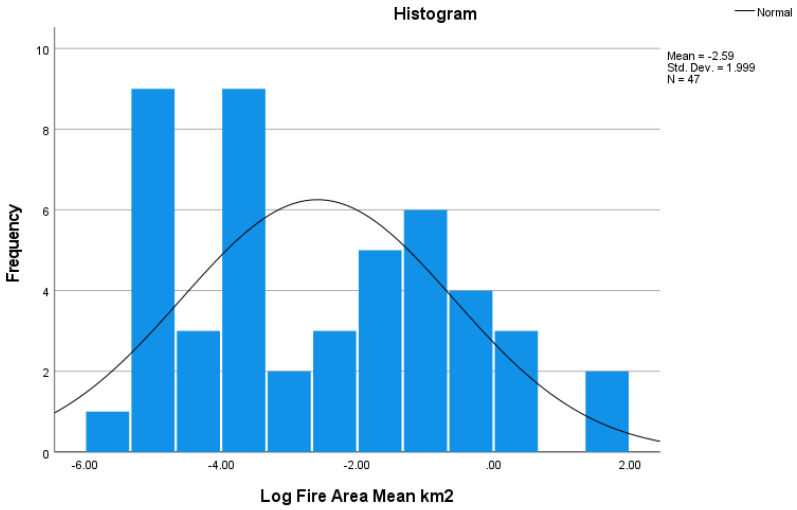

Appendix C – Larger Versions of Maps

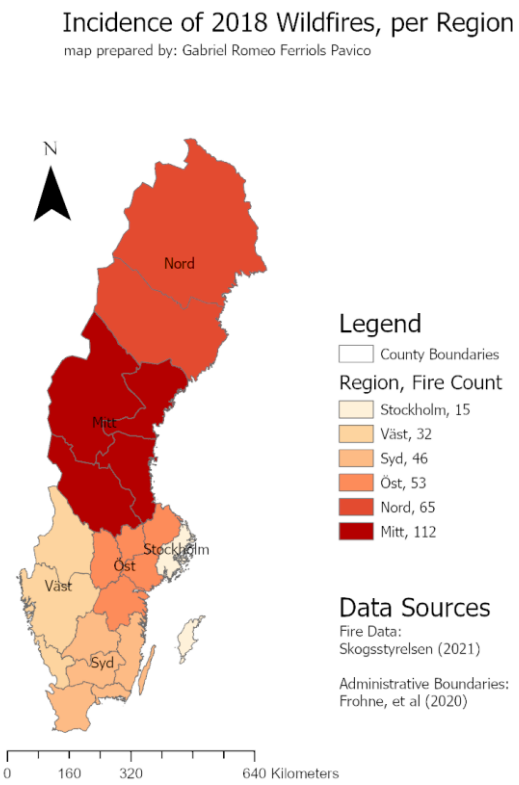

Figure 3: Incidence of 2018 Wildfires

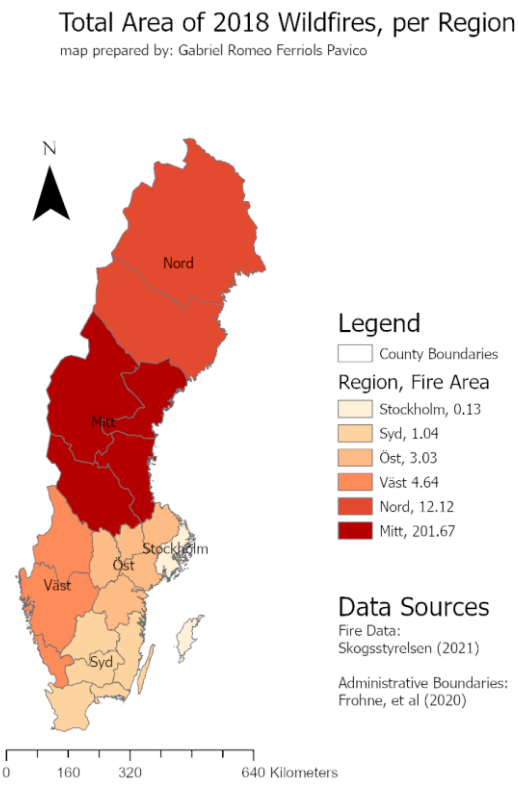

Figure 2: Total Area of 2018 Wildfires

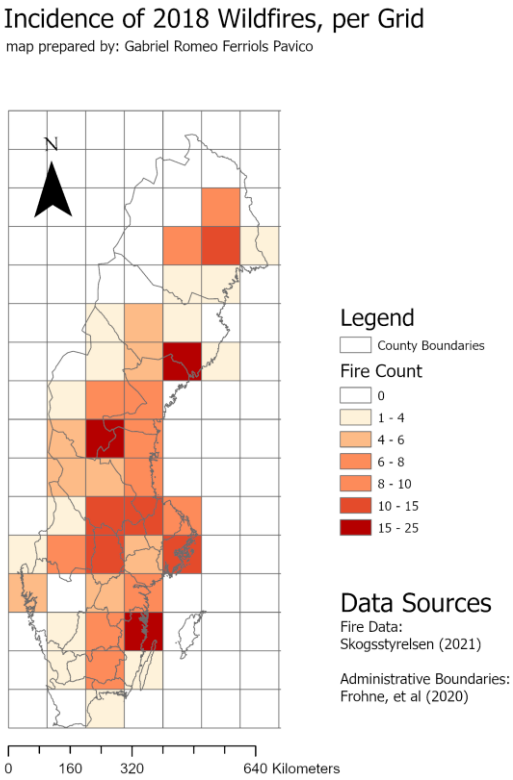

Figure 8: Incidence of 2018 Wildfires (Grid)

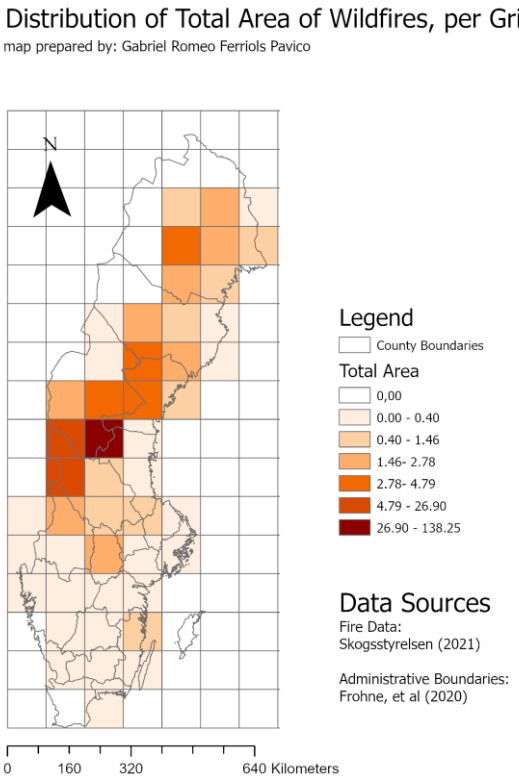

Figure 9: Total Area of Wildfires (Grid)

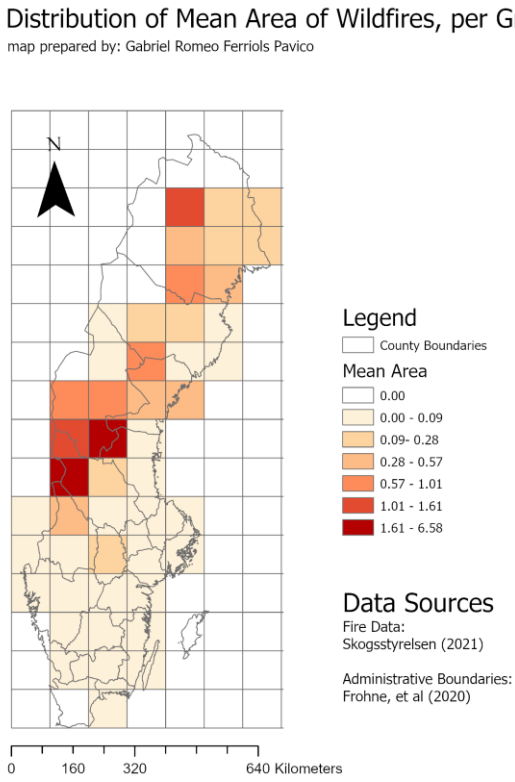

Figure 10: Mean Area of Wildfires (Grid)

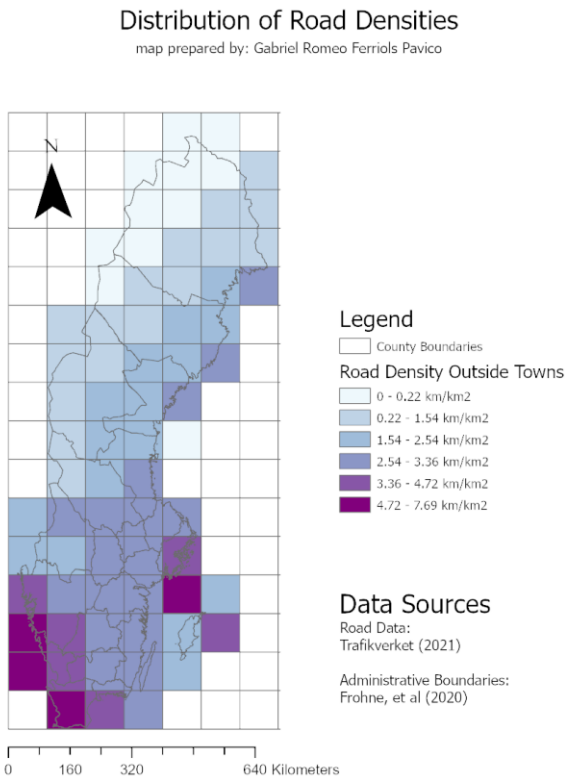

Figure 11: Distribution of Road Densities Outside Towns

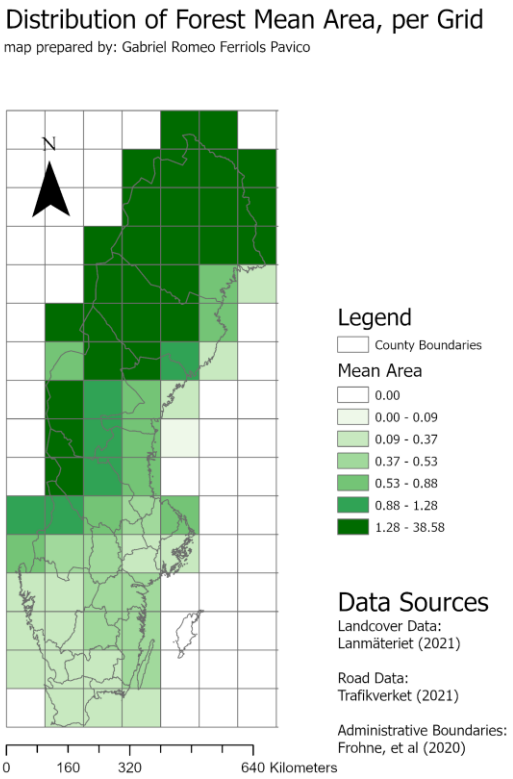

Figure 12: Distribution of Forest (Mean)

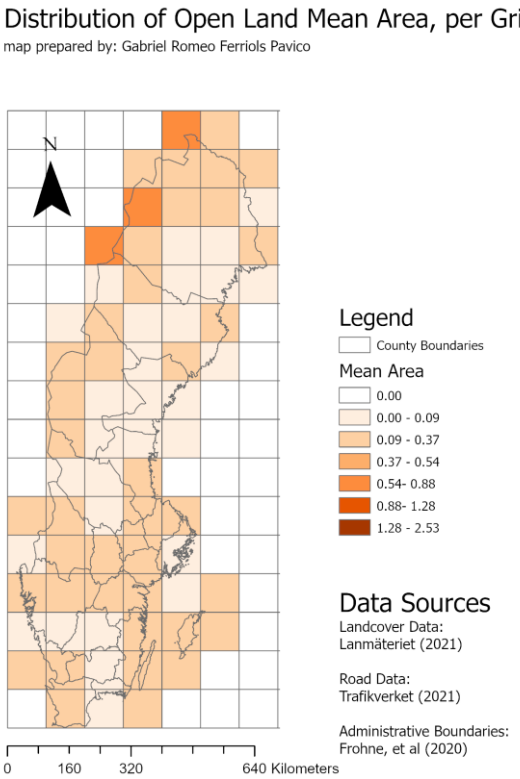

Figure 13: Distribution of Open Land (Mean)

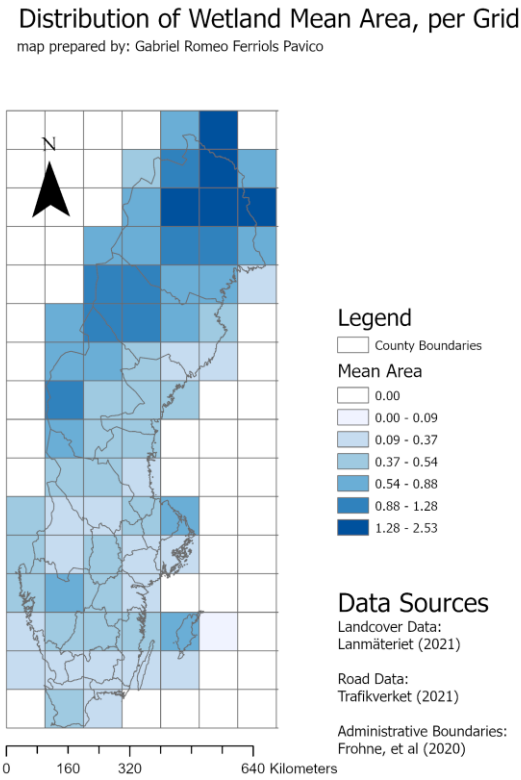

Figure 15: Distribution of Wetland (Mean)

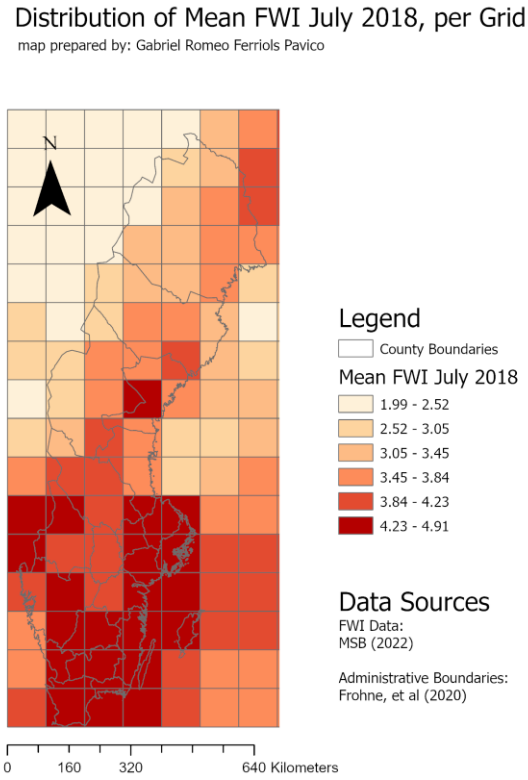

Figure 14: July FWI (Mean)

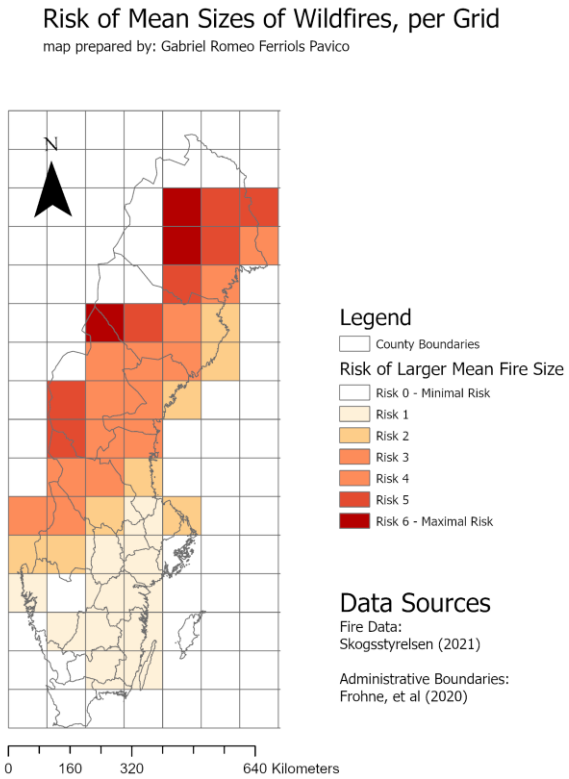

Figure 34: Risk of Mean Sizes of Wildfires

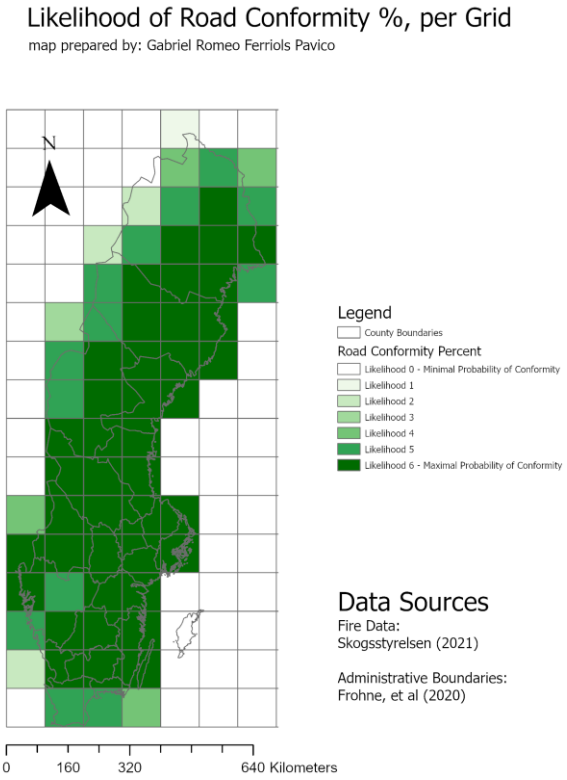

Figure 38: Likelihood of Road Conformity Percent

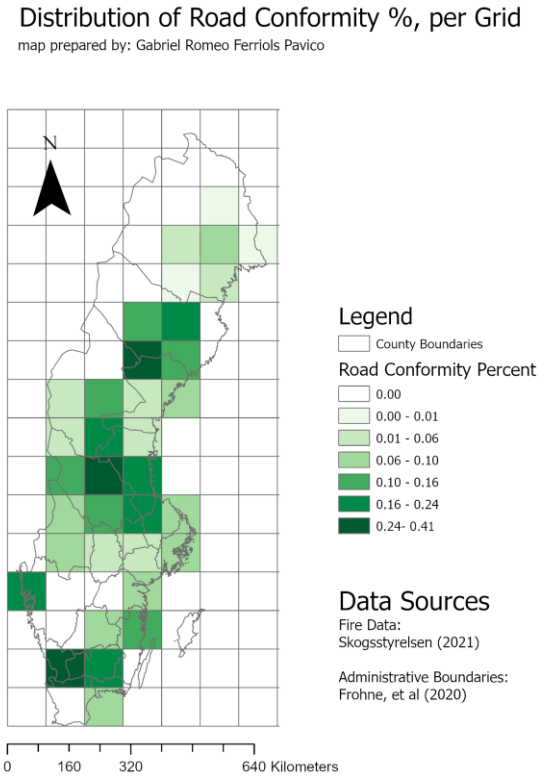

Figure 37: Distribution of Road Conformity Percent

Appendix D – Right to use of image

LUNDS UNIVERSITET

Gabriel Romeo Ferriols Pavico [redacted]

Användning av bilder från MSB rapporter

Kommunikation@msb.se <Kommunikation@msb.se> Fri, Oct 14, 2022 at 1:27 PM
To: Gabriel Romeo Ferriols Pavico <[redacted]

Hej!

Det går bra, använd bara MSB som källa.

Vänliga hälsningar,

[redacted]
Myndigheten för samhällsskydd och beredskap

Presstjänsten: 010-240 44 44
Epost: kommunikation@msb.se

Från: Gabriel Romeo Ferriols Pavico <[redacted]>
Skickat: den 14 oktober 2022 12:15
Till: Kommunikation@msb.se
Ämne: Användning av bilder från MSB rapporter

Hej!

Gabriel heter jag och jag håller på att skriva min masteruppsats om 2018 brandsäsong. Jag läste en rapport av Anders Granström med titeln Brandsommaren 2018 – Vad hände, och varför? https://rib.msb.se/filer/pdf/29059.pdf och undrar om jag kan få lov att använda en skiss från dokumentet?

Jag hoppas att ni kan hjälpa mig angående detta! Eller om ni har inget att göra med upphovsrätt, jag hoppas att ni kan koppla mig till enheten som sysslar med detta. Eller bör jag kontakta forskaren direkt?

Tack så hemskt mycket!

/Gabriel

Series from Lund University

Department of Physical Geography and Ecosystem Science

Master Thesis in Geographical Information Science

1. *Anthony Lawther:* The application of GIS-based binary logistic regression for slope failure susceptibility mapping in the Western Grampian Mountains, Scotland (2008).

2. *Rickard Hansen:* Daily mobility in Grenoble Metropolitan Region, France. Applied GIS methods in time geographical research (2008).

3. *Emil Bayramov:* Environmental monitoring of bio-restoration activities using GIS and Remote Sensing (2009).

4. *Rafael Villarreal Pacheco:* Applications of Geographic Information Systems as an analytical and visualization tool for mass real estate valuation: a case study of Fontibon District, Bogota, Columbia (2009).

5. *Siri Oestreich Waage:* a case study of route solving for oversized transport: The use of GIS functionalities in transport of transformers, as part of maintaining a reliable power infrastructure (2010).

6. *Edgar Pimiento:* Shallow landslide susceptibility – Modelling and validation (2010).

7. *Martina Schäfer:* Near real-time mapping of floodwater mosquito breeding sites using aerial photographs (2010).

8. *August Pieter van Waarden-Nagel:* Land use evaluation to assess the outcome of the programme of rehabilitation measures for the river Rhine in the Netherlands (2010).

9. *Samira Muhammad:* Development and implementation of air quality data mart for Ontario, Canada: A case study of air quality in Ontario using OLAP tool. (2010).

10. *Fredros Oketch Okumu*: Using remotely sensed data to explore spatial and temporal relationships between photosynthetic productivity of vegetation and malaria transmission intensities in selected parts of Africa (2011).

11. *Svajunas Plunge:* Advanced decision support methods for solving diffuse water pollution problems (2011).

12. *Jonathan Higgins:* Monitoring urban growth in greater Lagos: A case study using GIS to monitor the urban growth of Lagos 1990 - 2008 and produce future growth prospects for the city (2011).

13. *Mårten Karlberg:* Mobile Map Client API: Design and Implementation for Android (2011).

14. *Jeanette McBride:* Mapping Chicago area urban tree canopy using color infrared imagery (2011).

15. *Andrew Farina:* Exploring the relationship between land surface temperature and vegetation abundance for urban heat island mitigation in Seville, Spain (2011).

16. *David Kanyari*: Nairobi City Journey Planner: An online and a Mobile Application (2011).

17. *Laura V. Drews:* Multi-criteria GIS analysis for siting of small wind power plants - A case study from Berlin (2012).

18. *Qaisar Nadeem:* Best living neighborhood in the city - A GIS based multi criteria evaluation of ArRiyadh City (2012).

19. *Ahmed Mohamed El Saeid Mustafa:* Development of a photo voltaic building rooftop integration analysis tool for GIS for Dokki District, Cairo, Egypt (2012).

20. *Daniel Patrick Taylor*: Eastern Oyster Aquaculture: Estuarine Remediation via Site Suitability and Spatially Explicit Carrying Capacity Modeling in Virginia's Chesapeake Bay (2013).

21. *Angeleta Oveta Wilson:* A Participatory GIS approach to *unearthing* Manchester's Cultural Heritage '*gold mine'* (2013).

22. *Ola Svensson:* Visibility and Tholos Tombs in the Messenian Landscape: A Comparative Case Study of the Pylian Hinterlands and the Soulima Valley (2013).

23. *Monika Ogden:* Land use impact on water quality in two river systems in South Africa (2013).

24. *Stefan Rova:* A GIS based approach assessing phosphorus load impact on Lake Flaten in Salem, Sweden (2013).

25. *Yann Buhot:* Analysis of the history of landscape changes over a period of 200 years. How can we predict past landscape pattern scenario and the impact on habitat diversity? (2013).

26. *Christina Fotiou:* Evaluating habitat suitability and spectral heterogeneity models to predict weed species presence (2014).

27. *Inese Linuza:* Accuracy Assessment in Glacier Change Analysis (2014).

28. *Agnieszka Griffin:* Domestic energy consumption and social living standards: a GIS analysis within the Greater London Authority area (2014).

29. *Brynja Guðmundsdóttir:* Detection of potential arable land with remote sensing and GIS - A Case Study for Kjósarhreppur (2014).

30. *Oleksandr Nekrasov:* Processing of MODIS Vegetation Indices for analysis of agricultural droughts in the southern Ukraine between the years 2000-2012 (2014).

31. *Sarah Tressel:* Recommendations for a polar Earth science portal in the context of Arctic Spatial Data Infrastructure (2014).

32. *Caroline Gevaert:* Combining Hyperspectral UAV and Multispectral Formosat-2 Imagery for Precision Agriculture Applications (2014).

33. *Salem Jamal-Uddeen:* Using GeoTools to implement the multi-criteria evaluation analysis - weighted linear combination model (2014).

34. *Samanah Seyedi-Shandiz:* Schematic representation of geographical railway network at the Swedish Transport Administration (2014).

35. *Kazi Masel Ullah:* Urban Land-use planning using Geographical Information System and analytical hierarchy process: case study Dhaka City (2014).

36. *Alexia Chang-Wailing Spitteler:* Development of a web application based on MCDA and GIS for the decision support of river and floodplain rehabilitation projects (2014).

37. *Alessandro De Martino:* Geographic accessibility analysis and evaluation of potential changes to the public transportation system in the City of Milan (2014).

38. *Alireza Mollasalehi:* GIS Based Modelling for Fuel Reduction Using Controlled Burn in Australia. Case Study: Logan City, QLD (2015).

39. *Negin A. Sanati:* Chronic Kidney Disease Mortality in Costa Rica; Geographical Distribution, Spatial Analysis and Non-traditional Risk Factors (2015).

40. *Karen McIntyre:* Benthic mapping of the Bluefields Bay fish sanctuary, Jamaica (2015).

41. *Kees van Duijvendijk:* Feasibility of a low-cost weather sensor network for agricultural purposes: A preliminary assessment (2015).

42. *Sebastian Andersson Hylander:* Evaluation of cultural ecosystem services using GIS (2015).

43. *Deborah Bowyer:* Measuring Urban Growth, Urban Form and Accessibility as Indicators of Urban Sprawl in Hamilton, New Zealand (2015).

44. *Stefan Arvidsson:* Relationship between tree species composition and phenology extracted from satellite data in Swedish forests (2015).

45. *Damián Giménez Cruz*: GIS-based optimal localisation of beekeeping in rural Kenya (2016).

46. *Alejandra Narváez Vallejo:* Can the introduction of the topographic indices in LPJ-GUESS improve the spatial representation of environmental variables? (2016).

47. *Anna Lundgren:* Development of a method for mapping the highest coastline in Sweden using breaklines extracted from high resolution digital elevation models (2016).

48. *Oluwatomi Esther Adejoro:* Does location also matter? A spatial analysis of social achievements of young South Australians (2016).

49. *Hristo Dobrev Tomov:* Automated temporal NDVI analysis over the Middle East for the period 1982 - 2010 (2016).

50. *Vincent Muller:* Impact of Security Context on Mobile Clinic Activities A GIS Multi Criteria Evaluation based on an MSF Humanitarian Mission in Cameroon (2016).

51. *Gezahagn Negash Seboka:* Spatial Assessment of NDVI as an Indicator of Desertification in Ethiopia using Remote Sensing and GIS (2016).

52. *Holly Buhler:* Evaluation of Interfacility Medical Transport Journey Times in Southeastern British Columbia. (2016).

53. *Lars Ole Grottenberg*: Assessing the ability to share spatial data between emergency management organisations in the High North (2016).

54. *Sean Grant:* The Right Tree in the Right Place: Using GIS to Maximize the Net Benefits from Urban Forests (2016).

55. *Irshad Jamal:* Multi-Criteria GIS Analysis for School Site Selection in Gorno-Badakhshan Autonomous Oblast, Tajikistan (2016).

56. *Fulgencio Sanmartín:* Wisdom-volkano: A novel tool based on open GIS and time-series visualization to analyse and share volcanic data (2016).

57. *Nezha Acil:* Remote sensing-based monitoring of snow cover dynamics and its influence on vegetation growth in the Middle Atlas Mountains (2016).

58. *Julia Hjalmarsson:* A Weighty Issue: Estimation of Fire Size with Geographically Weighted Logistic Regression (2016).

59. *Mathewos Tamiru Amato:* Using multi-criteria evaluation and GIS for chronic food and nutrition insecurity indicators analysis in Ethiopia (2016).

60. *Karim Alaa El Din Mohamed Soliman El Attar:* Bicycling Suitability in Downtown, Cairo, Egypt (2016).

61. *Gilbert Akol Echelai:* Asset Management: Integrating GIS as a Decision Support Tool in Meter Management in National Water and Sewerage Corporation (2016).

62. *Terje Slinning:* Analytic comparison of multibeam echo soundings (2016).

63. *Gréta Hlín Sveinsdóttir:* GIS-based MCDA for decision support: A framework for wind farm siting in Iceland (2017).

64. *Jonas Sjögren:* Consequences of a flood in Kristianstad, Sweden: A GIS-based analysis of impacts on important societal functions (2017).

65. *Nadine Raska:* 3D geologic subsurface modelling within the Mackenzie Plain, Northwest Territories, Canada (2017).

66. *Panagiotis Symeonidis*: Study of spatial and temporal variation of atmospheric optical parameters and their relation with PM 2.5 concentration over Europe using GIS technologies (2017).

67. *Michaela Bobeck:* A GIS-based Multi-Criteria Decision Analysis of Wind Farm Site Suitability in New South Wales, Australia, from a Sustainable Development Perspective (2017).

68. *Raghdaa Eissa*: Developing a GIS Model for the Assessment of Outdoor Recreational Facilities in New Cities Case Study: Tenth of Ramadan City, Egypt (2017).

69. *Zahra Khais Shahid*: Biofuel plantations and isoprene emissions in Svea and Götaland (2017).

70. *Mirza Amir Liaquat Baig*: Using geographical information systems in epidemiology: Mapping and analyzing occurrence of diarrhea in urban - residential area of Islamabad, Pakistan (2017).

71. *Joakim Jörwall*: Quantitative model of Present and Future well-being in the EU-28: A spatial Multi-Criteria Evaluation of socioeconomic and climatic comfort factors (2017).

72. *Elin Haettner*: Energy Poverty in the Dublin Region: Modelling Geographies of Risk (2017).

73. *Harry Eriksson*: Geochemistry of stream plants and its statistical relations to soil- and bedrock geology, slope directions and till geochemistry. A GIS-analysis of small catchments in northern Sweden (2017).

74. *Daniel Gardevärn:* PPGIS and Public meetings – An evaluation of public participation methods for urban planning (2017).

75. *Kim Friberg:* Sensitivity Analysis and Calibration of Multi Energy Balance Land Surface Model Parameters (2017).

76. *Viktor Svanerud:* Taking the bus to the park? A study of accessibility to green areas in Gothenburg through different modes of transport (2017).

77. *Lisa-Gaye Greene*: Deadly Designs: The Impact of Road Design on Road Crash Patterns along Jamaica's North Coast Highway (2017).

78. *Katarina Jemec Parker*: Spatial and temporal analysis of fecal indicator bacteria concentrations in beach water in San Diego, California (2017).

79. *Angela Kabiru*: An Exploratory Study of Middle Stone Age and Later Stone Age Site Locations in Kenya's Central Rift Valley Using Landscape Analysis: A GIS Approach (2017).

80. *Kristean Björkmann*: Subjective Well-Being and Environment: A GIS-Based Analysis (2018).

81. *Williams Erhunmonmen Ojo*: Measuring spatial accessibility to healthcare for people living with HIV-AIDS in southern Nigeria (2018).

82. *Daniel Assefa*: Developing Data Extraction and Dynamic Data Visualization (Styling) Modules for Web GIS Risk Assessment System (WGRAS). (2018).

83. *Adela Nistora*: Inundation scenarios in a changing climate: assessing potential impacts of sea-level rise on the coast of South-East England (2018).

84. *Marc Seliger*: Thirsty landscapes - Investigating growing irrigation water consumption and potential conservation measures within Utah's largest master-planned community: Daybreak (2018).

85. *Luka Jovičić*: Spatial Data Harmonisation in Regional Context in Accordance with INSPIRE Implementing Rules (2018).

86. *Christina Kourdounouli*: Analysis of Urban Ecosystem Condition Indicators for the Large Urban Zones and City Cores in EU (2018).

87. *Jeremy Azzopardi*: Effect of distance measures and feature representations on distance-based accessibility measures (2018).

88. *Patrick Kabatha*: An open source web GIS tool for analysis and visualization of elephant GPS telemetry data, alongside environmental and anthropogenic variables (2018).

89. *Richard Alphonce Giliba*: Effects of Climate Change on Potential Geographical Distribution of Prunus africana (African cherry) in the Eastern Arc Mountain Forests of Tanzania (2018).

90. *Eiður Kristinn Eiðsson*: Transformation and linking of authoritative multi-scale geodata for the Semantic Web: A case study of Swedish national building data sets (2018).

91. *Niamh Harty*: HOP!: a PGIS and citizen science approach to monitoring the condition of upland paths (2018).

92. *José Estuardo Jara Alvear*: Solar photovoltaic potential to complement hydropower in Ecuador: A GIS-based framework of analysis (2018).

93. *Brendan O'Neill*: Multicriteria Site Suitability for Algal Biofuel Production Facilities (2018).

94. *Roman Spataru*: Spatial-temporal GIS analysis in public health – a case study of polio disease (2018).

95. *Alicja Miodońska*: Assessing evolution of ice caps in Suðurland, Iceland, in years 1986 - 2014, using multispectral satellite imagery (2019).

96. *Dennis Lindell Schettini*: A Spatial Analysis of Homicide Crime's Distribution and Association with Deprivation in Stockholm Between 2010-2017 (2019).

97. *Damiano Vesentini*: The Po Delta Biosphere Reserve: Management challenges and priorities deriving from anthropogenic pressure and sea level rise (2019).

98. *Emilie Arnesten*: Impacts of future sea level rise and high water on roads, railways and environmental objects: a GIS analysis of the potential effects of increasing sea levels and highest projected high water in Scania, Sweden (2019).

99. *Syed Muhammad Amir Raza*: Comparison of geospatial support in RDF stores: Evaluation for ICOS Carbon Portal metadata (2019).

100. *Hemin Tofiq*: Investigating the accuracy of Digital Elevation Models from UAV images in areas with low contrast: A sandy beach as a case study (2019).

101. *Evangelos Vafeiadis*: Exploring the distribution of accessibility by public transport using spatial analysis. A case study for retail concentrations and public hospitals in Athens (2019).

102. *Milan Sekulic*: Multi-Criteria GIS modelling for optimal alignment of roadway by-passes in the Tlokweng Planning Area, Botswana (2019).

103. *Ingrid Piirisaar*: A multi-criteria GIS analysis for siting of utility-scale photovoltaic solar plants in county Kilkenny, Ireland (2019).

104. *Nigel Fox*: Plant phenology and climate change: possible effect on the onset of various wild plant species' first flowering day in the UK (2019).

105. *Gunnar Hesch*: Linking conflict events and cropland development in Afghanistan, 2001 to 2011, using MODIS land cover data and Uppsala Conflict Data Programme (2019).

106. *Elijah Njoku*: Analysis of spatial-temporal pattern of Land Surface Temperature (LST) due to NDVI and elevation in Ilorin, Nigeria (2019).

107. *Katalin Bunyevácz*: Development of a GIS methodology to evaluate informal urban green areas for inclusion in a community governance program (2019).

108. *Paul dos Santos*: Automating synthetic trip data generation for an agent-based simulation of urban mobility (2019).

109. *Robert O' Dwyer*: Land cover changes in Southern Sweden from the mid-Holocene to present day: Insights for ecosystem service assessments (2019).

110. *Daniel Klingmyr*: Global scale patterns and trends in tropospheric NO2 concentrations (2019).

111. *Marwa Farouk Elkabbany*: Sea Level Rise Vulnerability Assessment for Abu Dhabi, United Arab Emirates (2019).

112. *Jip Jan van Zoonen*: Aspects of Error Quantification and Evaluation in Digital Elevation Models for Glacier Surfaces (2020).

113. *Georgios Efthymiou*: The use of bicycles in a mid-sized city – benefits and obstacles identified using a questionnaire and GIS (2020).

114. *Haruna Olayiwola Jimoh*: Assessment of Urban Sprawl in MOWE/IBAFO Axis of Ogun State using GIS Capabilities (2020).

115. *Nikolaos Barmpas Zachariadis*: Development of an iOS, Augmented Reality for disaster management (2020).

116. *Ida Storm*: ICOS Atmospheric Stations: Spatial Characterization of CO2 Footprint Areas and Evaluating the Uncertainties of Modelled CO2 Concentrations (2020).

117. *Alon Zuta*: Evaluation of water stress mapping methods in vineyards using airborne thermal imaging (2020).

118. *Marcus Eriksson*: Evaluating structural landscape development in the municipality Upplands-Bro, using landscape metrics indices (2020).

119. *Ane Rahbek Vierø*: Connectivity for Cyclists? A Network Analysis of Copenhagen's Bike Lanes (2020).

120. *Cecilia Baggini*: Changes in habitat suitability for three declining Anatidae species in saltmarshes on the Mersey estuary, North-West England (2020).

121. *Bakrad Balabanian*: Transportation and Its Effect on Student Performance (2020).

122. *Ali Al Farid*: Knowledge and Data Driven Approaches for Hydrocarbon Microseepage Characterizations: An Application of Satellite Remote Sensing (2020).

123. *Bartlomiej Kolodziejczyk*: Distribution Modelling of Gene Drive-Modified Mosquitoes and Their Effects on Wild Populations (2020).

124. *Alexis Cazorla*: Decreasing organic nitrogen concentrations in European water bodies - links to organic carbon trends and land cover (2020).

125. *Kharid Mwakoba*: Remote sensing analysis of land cover/use conditions of community-based wildlife conservation areas in Tanzania (2021).

126. *Chinatsu Endo*: Remote Sensing Based Pre-Season Yellow Rust Early Warning in Oromia, Ethiopia (2021).

127. *Berit Mohr*: Using remote sensing and land abandonment as a proxy for long-term human out-migration. A Case Study: Al-Hassakeh Governorate, Syria (2021).

128. *Kanchana Nirmali Bandaranayake*: Considering future precipitation in delineation locations for water storage systems - Case study Sri Lanka (2021).

129. *Emma Bylund*: Dynamics of net primary production and food availability in the aftermath of the 2004 and 2007 desert locust outbreaks in Niger and Yemen (2021).

130. *Shawn Pace*: Urban infrastructure inundation risk from permanent sea-level rise scenarios in London (UK), Bangkok (Thailand) and Mumbai (India): A comparative analysis (2021).

131. *Oskar Evert Johansson*: The hydrodynamic impacts of Estuarine Oyster reefs, and the application of drone technology to this study (2021).

132. *Pritam Kumarsingh*: A Case Study to develop and test GIS/SDSS methods to assess the production capacity of a Cocoa Site in Trinidad and Tobago (2021).

133. *Muhammad Imran Khan*: Property Tax Mapping and Assessment using GIS (2021).

134. *Domna Kanari*: Mining geosocial data from Flickr to explore tourism patterns: The case study of Athens (2021).

135. *Mona Tykesson Klubien*: Livestock-MRSA in Danish pig farms (2021).

136. *Ove Njøten*: Comparing radar satellites. Use of Sentinel-1 leads to an increase in oil spill alerts in Norwegian waters (2021).

137. *Panagiotis Patrinos*: Change of heating fuel consumption patterns produced by the economic crisis in Greece (2021).

138. *Lukasz Langowski*: Assessing the suitability of using Sentinel-1A SAR multi-temporal imagery to detect fallow periods between rice crops (2021).

139. *Jonas Tillman*: Perception accuracy and user acceptance of legend designs for opacity data mapping in GIS (2022).

140. *Gabriela Olekszyk*: ALS (Airborne LIDAR) accuracy: Can potential low data quality of ground points be modelled/detected? Case study of 2016 LIDAR capture over Auckland, New Zealand (2022).

141. *Luke Aspland*: Weights of Evidence Predictive Modelling in Archaeology (2022).

142. *Luís Fareleira Gomes*: The influence of climate, population density, tree species and land cover on fire pattern in mainland Portugal (2022).

143. *Andreas Eriksson*: Mapping Fire Salamander (Salamandra salamandra) Habitat Suitability in Baden-Württemberg with Multi-Temporal Sentinel-1 and Sentinel-2 Imagery (2022).

144. *Lisbet Hougaard Baklid*: Geographical expansion rate of a brown bear population in Fennoscandia and the factors explaining the directional variations (2022).

145. *Victoria Persson*: Mussels in deep water with climate change: Spatial distribution of mussel (Mytilus galloprovincialis) growth offshore in the French Mediterranean with respect to climate change scenario RCP 8.5 Long Term and Integrated Multi-Trophic Aquaculture (IMTA) using Dynamic Energy Budget (DEB) modelling (2022).

146. *Benjamin Bernard Fabien Gérard Borgeais*: Implementing a multi-criteria GIS analysis and predictive modelling to locate Upper Palaeolithic decorated caves in the Périgord noir, France (2022).

147. *Bernat Dorado-Guerrero*: Assessing the impact of post-fire restoration interventions using spectral vegetation indices: A case study in El Bruc, Spain (2022).

148. *Ignatius Gabriel Aloysius Maria Perera*: The Influence of Natural Radon Occurrence on the Severity of the COVID-19 Pandemic in Germany: A Spatial Analysis (2022).

149. *Mark Overton*: An Analysis of Spatially-enabled Mobile Decision Support Systems in a Collaborative Decision-Making Environment (2022).

150. *Viggo Lunde*: Analysing methods for visualizing time-series datasets in open-source web mapping (2022).

151. *Johan Viscarra Hansson*: Distribution Analysis of Impatiens glandulifera in Kronoberg County and a Pest Risk Map for Alvesta Municipality (2022).

152. *Vincenzo Poppiti*: GIS and Tourism: Developing strategies for new touristic flows after the Covid-19 pandemic (2022).

153. *Henrik Hagelin*: Wildfire growth modelling in Sweden - A suitability assessment of available data (2023).

154. *Gabriel Romeo Ferriols Pavico*: Where there is road, there is fire (influence): An exploratory study on the influence of roads in the spatial patterns of Swedish wildfires of 2018 (2023).